

Copyright

by

Austin Francis Rechner

2020

**The Thesis Committee for Austin Francis Rechner
Certifies that this is the approved version of the following Thesis:**

**A Comparison of Transpiration Rates from Three Semi-Arid Tree
Species in Response to Partial Stand Clearing**

**APPROVED BY
SUPERVISING COMMITTEE:**

Ashley Matheny, Supervisor
Daniella Rempe
Meinhard Cardenas

**A Comparison of Transpiration Rates from Three Semi-Arid Tree
Species in Response to Partial Stand Clearing**

by

Austin Francis Rechner

Thesis

Presented to the Faculty of the Graduate School of

The University of Texas at Austin

in Partial Fulfillment

of the Requirements

for the Degree of

Master of Science in Geological Sciences

The University of Texas at Austin

August 2020

Abstract

A Comparison of Transpiration Rates from Three Semi-Arid Tree Species in Response to Partial Stand Clearing

Austin Francis Rechner, M. S. GeoSci
The University of Texas at Austin, 2020

Supervisor: Ashley Matheny

As precipitation and temperature patterns continue to shift in response to climate change, total water availability including soil and surface waters are likewise altered. In central and west Texas, a common land management practice thought to increase surface water quantities and spring flow is the removal of *Juniperus ashei* commonly referred to as ashe juniper or cedar. Vegetative cover impacts the local water cycle through multiple feedback mechanisms including extraction of soil water by roots, and transpiration of water vapor back into the atmosphere. Through transpiration, plants exchange water for carbon from the atmosphere. This study aims to determine changes in transpiration rates pre- and post partial removal of ashe juniper (*J. ashei*) in a semi-arid forest located near Rocksprings, Texas using micrometeorological and sap flux data. We compared transpiration rates between three tree species - pinyon pine (*Pinus remota*), lacey oak (*Quercus laceyi*), and ashe juniper (*J. ashei*) under a variety of environmental conditions. Sap flow data revealed that ashe juniper used less water per day than the pines but more than the oaks. Transpiration rates increased after juniper removal with pines still transpiring the most water followed by juniper, and oaks using the least. Additionally, it was found that pine trees located at lower elevations transpired more than individuals at

higher elevations. By contrast, oak and juniper trees showed higher transpiration rates at higher elevations. An enhanced understanding of vegetation-climate interactions will provide key information for land management best practices to ensure resource resilience in the face of changing climate.

Table of Contents

List of Tables	ix
List of Figures.....	x
Chapter 1: Introduction.....	1
1.1 Climate Dynamics.....	1
1.2 Woody Plant Encroachment	2
1.3 <i>Juniperus ashei</i> encroachment in central Texas	3
1.4 Juniper Clearing From The Texas Landscape	5
Chapter 2: Methods.....	8
2.1 Field Site Description	8
2.2 Sap Flux	11
2.2.1 Sensor Theory	11
2.2.2 Sensor Construction	12
2.3 Field Site Setup.....	13
2.3.1 Sap Flux Sensor Installation	14
2.4 Tree Cores.....	16
2.5 Tree Crown Area and Heights	17
2.6 Leaf Water Potentials.....	18
2.7 Hydro-Meteorological Monitoring Station.....	19
2.8 Data Processing.....	19
2.8.1 Hydro-meteorological Data Processing	19
2.8.2 Sap Flux Data Processing	20

Chapter 3: Results	22
3.1 Site Meteorology and Interannual variability	22
3.2 Pre- and Post-clearing Comparisons.....	26
3.2.1 13-Day Similar Hydro-meteorological Conditions Comparison	26
3.2.2 Sap Flux Compared During Changing Soil Conditions.....	29
3.3 Diurnal patterns.....	32
3.3.1 Diurnal Patterns among Tree Size Classifications.....	33
3.3.1a Juniper	33
3.3.1b Pine	34
3.3.1c Oak	35
3.3.2 Wet and Dry Conditions	35
3.3.2a Juniper	36
3.3.2b Pine	37
3.3.2c Oak	38
3.3.3 Transpiration responses to partial clearing of <i>J. ashei</i>	39
3.3.4 Elevation change and sap flux	41
3.3.4a Juniper	41
3.3.4b Pine	41
3.3.4c Oak	42
3.4 Leaf Water Potential Measurements.....	43
3.4.1 Leaf Water Potential vs. Vapor Pressure Deficient	43
3.4.2 Leaf Water Potential and Soil Water Content.....	47
3.5 Visual Increases in Spring Water.....	49

Chapter 4: Discussion	50
4.1 Pre- Post- Clearing Transpiration Changes	50
4.2 Transpiration Response To Environmental Conditions.....	52
4.2.1 Diurnal Sap Flux Response to Environmental Conditions	52
4.2.2 Vegetation Response to Drought	53
4.3 Transpiration Compared to Elevation, Hillslope Hydrology and Rooting Depth.....	55
4.3.1 Elevation Comparisons	55
4.3.2 Hillslope Hydrology.....	55
4.3.3 Rooting Depth.....	56
4.4 Spring flow Changes From Juniper Removal.....	57
Chapter 5: Conclusions	59
Appendix.....	61
References.....	63

List of Tables

Table 1: Acceptable resistance ranges for wired connections during sap flux sensor assembly.....	13
Table 2: Data related to trees with sap flux sensors.....	14
Table 3: Equations for the line of best fit for each species from Figure 6.....	17
Table 4: Mean hydro-meteorological parameters for DOY 120 - 300 for 2018 and 2019. Values in parenthesis are the standard deviations for the growing period selected. The third column is the percent change in averages between 2018 and 2019.	23
Table 5: Comparison of hydro-meteorological conditions for a 13-day period representing preclearing (2018) and post clearing (2019). The two periods are within ~20% of each other in terms of all parameters below.....	26
Table 6: Comparison of transpiration rate for pre- and post-clearing 13-day period.	29
Table 7: Equations of best fit and their R ² values for 2018 and 2019 comparison of sap flux and SWC shown in Figure 11. The best fit is a logarithmic curve.....	32
Table 8: Mean hydro-meteorological values for seven day wet (SWC > 0.3 m ³ H ₂ O m ⁻³ soil) and dry periods (SWC < 0.2 m ³ H ₂ O m ⁻³ soil). The standard deviation of the mean values is given in parentheses. Percent change was calculated based on the difference between wet conditions and dry conditions.	36
Table 9: Average transpiration rates pre- (2018), postclearing (2019), and the average of both years by species and medium (13 cm ≤ DBH ≤ 24 cm) and large (DBH > 24 cm) size classifications.....	40
Table 10: Leaf water measurements taken in triplicate and averaged with the standard deviation in the parentheses. Measurements that are italicized were taken during overcast conditions, and evening measurements were conducted after the sun had set but prior to full dark conditions.	45
Table 11: Slope values for leaf water potential plotted against VPD for each sampling period. Relationships that were not significant are shown as (-).	47
Table 12: Slope values for leaf water potential plotted against SWC for each sampling period. Relationships that were not significant are shown as (-).	49

List of Figures

Figure 1: The contour map on the top is an extended view of the surrounding topography with 5-meter contours. The red box within the top image is the sap flux site. The bottom image shows the locations of the different oaks (blue triangles), pines (green squares), junipers (orange circles) with sap flux sensors installed with 1-meter contours. The gray shadow in the top right is the area where the clearing happened in the spring of 2019. Table 2 shows the descriptions of the trees labeled in this figure. 10

Figure 2: Example of a hand-made thermal dissipation probe sap flux sensor with the heating wire located on the right needle. 11

Figure 3: Sap flux sensor installation. Top needle has the heating coil, and the bottom measures the reference temperature. 15

Figure 4: Sap flux sensors installed and covered by reflective thermal insulation. 16

Figure 5: Sapwood area is linearly related to diameter at breast height (DBH) for all three species. The dotted lines are lines of best fit. 17

Figure 6: 2018 time series of hydro-meteorological and sap flux data at a half-hourly time step. The top plot shows a strong relationship between precipitation and SWC. The second plot (B) shows temperature and VPD. The bottom three plots (C, D, E) shows the average sap flux by species from DOY 120-365 with a gray dashed line for reference between species and years (Figure 7). 24

Figure 7: 2019 yearly time series of meteorological and sap flux data consisting of half hour averages. The bottom three plots (C, D, E) shows the average sap flux by species. The bottom plot shows the average sap flux by species. The red box over DOY 84-106, indicates the period of active removal of junipers, and the gray dashed line is for comparisons between species and years (Figure 6). 25

Figure 8: 2018, 13-day period before juniper clearing with soil conditions continuously getting drier (A). The bottom three plots (C, D, and E) show sap flux for each species by medium ($13 \text{ cm} \leq \text{DBH} \leq 24 \text{ cm}$) and large ($\text{DBH} > 24 \text{ cm}$) size classifications. The gray dashed line (C, D, and E) is a reference to compare between species and year (Figure 9). 27

Figure 9: 2019, 13-day period post juniper clearing with soil conditions continuously getting drier (A). The bottom three plots (C, D, and E) show sap flux for each species by medium ($13 \text{ cm} \leq \text{DBH} \leq 24 \text{ cm}$) and large ($\text{DBH} > 24 \text{ cm}$) size classifications. The gray dashed line (C, D, and E) is a reference to compare between species and year (Figure 8). 28

Figure 10: Average daily sap flux values compared with average daily SWC for DOY 120-300 in 2018 (A) and 2019 (B) for oak (blue), pine (green), and juniper (orange). The dotted lines represent the logarithmic line of best fit for each species. 31

Figure 11: Average instantaneous sap flux over diurnal period by species for 2018 (A) and 2019 (B) from DOY 120-300. 33

Figure 12: Average instantaneous sap flux over diurnal period for juniper from 2018 (A) and 2019 (B) DOY 120-300 by medium ($13 \text{ cm} \leq \text{DBH} \leq 24 \text{ cm}$) and large ($\text{DBH} > 24 \text{ cm}$) size classifications. 34

Figure 13: Average instantaneous sap flux over diurnal period for pines from 2018 (A) and 2019 (B) DOY 120-300 by medium ($13 \text{ cm} \leq \text{DBH} \leq 24 \text{ cm}$) and large ($\text{DBH} > 24 \text{ cm}$) size classifications. 34

Figure 14: Average instantaneous sap flux over diurnal period for oaks from 2018 (A) and 2019 (B) DOY 120-300 by medium ($13 \text{ cm} \leq \text{DBH} \leq 24 \text{ cm}$) and large ($\text{DBH} > 24 \text{ cm}$) size classifications. 35

Figure 15: Average instantaneous sap flux over diurnal period for junipers during 7-day period for dry conditions when $\text{SWC} < 0.2 \text{ m}^3\text{H}_2\text{O m}^{-3}$ (A) and wet conditions when $\text{SWC} > 0.3 \text{ m}^3\text{H}_2\text{O m}^{-3}$ (B) by medium ($13 \text{ cm} \leq \text{DBH} \leq 24 \text{ cm}$) and large ($\text{DBH} > 24 \text{ cm}$) size classifications. 37

Figure 16: Average instantaneous sap flux over diurnal period for pines during 7-day period for dry conditions when $\text{SWC} < 0.2 \text{ m}^3\text{H}_2\text{O m}^{-3}$ (A) and wet conditions when $\text{SWC} > 0.3 \text{ m}^3\text{H}_2\text{O m}^{-3}$ (B) by medium ($13 \text{ cm} \leq \text{DBH} \leq 24 \text{ cm}$) and large ($\text{DBH} > 24 \text{ cm}$) size classifications..... 38

Figure 17: Average instantaneous sap flux over diurnal period for oaks during 7-day period for dry conditions when $\text{SWC} < 0.2 \text{ m}^3\text{H}_2\text{O m}^{-3}$ (A) and wet conditions when $\text{SWC} > 0.3 \text{ m}^3\text{H}_2\text{O m}^{-3}$ (B) by medium ($13 \text{ cm} \leq \text{DBH} \leq 24 \text{ cm}$) and large ($\text{DBH} > 24 \text{ cm}$) size classifications. 39

Figure 18: Elevation influences on diurnal sap flux patterns for an up slope tree (Juniper 10) elevation 637.3 m, and a down slope tree (Juniper 7) elevation 631.5 m during 2018 (A) and 2019 (B). 41

Figure 19: Elevation influences on diurnal sap flux patterns for an up slope tree (Pine 6) elevation (638.5m), and a down slope tree (Pine 1) elevation (636.9 m) during 2018 (A) and 2019 (B) with a one hour moving average applied. 42

Figure 20: Elevation influences on diurnal sap flux patterns for an up slope tree (Oak 3) elevation 638.3 m, and a down slope tree (Oak 1) elevation 637.3 m during 2018 (A) and 2019 (B). 43

Figure 21: Leaf water potential (ψ_L) compared with atmospheric demand for water vapor (VPD). The pine, oak, and juniper are located at similar elevations in the upper portion of the slope, and “Juniper Low” was located at the bottom of the hillslope. The number (n) of measurements for each sampling period and tree is given in the top right of each plot. Significant P and R^2 values were added to each plot..... 46

Figure 22: ψ_L as compared to SWC. The pine, oak, and juniper are located at similar elevations in the upper portion of the slope, and “Juniper Low” was located at the bottom of the hillslope. The number (n) of measurements for each sampling period and tree is given in the top right of each plot. Significant P and R^2 values were added to each plot. 48

Figure 23: The average instantaneous sap flux over a diurnal period (dark orange) for juniper trees as seen in Figure 11 for 2018 (A) and 2019 (B) from DOY 120-300. The ten light orange lines are representative of varying patterns for diurnal curves from an individual tree responding to environmental conditions..... 61

Figure 24: The average instantaneous sap flux over a diurnal period (dark green) for pine trees as seen in Figure 11 for 2018 (A) and 2019 (B) from DOY 120-300. The ten light

green lines are representative of varying patterns for diurnal curves from an individual tree responding to environmental conditions. 61

Figure 25: The average instantaneous sap flux over a diurnal period (dark blue) for oak trees as seen in Figure 11 for 2018 (A) and 2019 (B) from DOY 120-300. The ten light blue lines are representative of varying patterns for diurnal curves from an individual tree responding to environmental conditions. 62

Chapter 1: Introduction

1.1 CLIMATE DYNAMICS

Terrestrial ecosystems play a central role in a number of climatic feedback loops via vegetation dynamics (Oki & Kanae, 2006). For example, as plants take in CO₂ from the atmosphere for photosynthesis, they release water vapor into the air. This release of water vapor, or transpiration, raises humidity, lowers the temperature, and ultimately helps generate cloud cover through rewetting of the atmospheric boundary layer. However, when the supply of water from the soil is reduced, plants prevent desiccation by shutting the leaf pores, stomata, leaf pores that regulate plant gas exchange, to reduce water loss through transpiration in order to prevent desiccation. In this circumstance, the solar energy that was previously evaporating transpired water into the atmosphere, latent heat, now warms the air as sensible heat in the absence of transpired water. Transpiration is also major flux in the hydrologic cycle, serving as a link between the subsurface and the atmosphere. It comprises 60-80% of evapotranspiration and contributes 39% of terrestrial precipitation globally (Schlesinger & Jasechko, 2014). Transpiration accounts for ~62,000 km³ of water recycling from the land surface to the atmosphere each year (Jasechko et al., 2013).

Climate change induced intensification of the global hydrologic cycle is predicted to lead to increases in extreme events such as flooding and droughts (Chapter2, IPCC). Intense precipitation events and droughts both will have major consequences on plant communities. Droughts apply two environmental stresses to plants decreased soil moisture and an increase in vapor pressure deficit. The increased water stress can result in cavitation. Cavitation is when water tension becomes high causing dissolved gas to form a bubble which blocks the xylem and prevents water movement and even death if prolonged drought occurs (Sperry et al., 1988). Trees, such as oaks, prevent cavitation by regulating their

stomata, closing them as soil water content dries in times of sparse precipitation as a defense against xylem cavitation (Tyree & Cochard, 1996). Stomata closure may prevent water stress but will induce carbon starvation from the lack of CO₂ coming into the leaf and will eventually lead to mortality (McDowell et al., 2008). Intense and more frequent precipitation and flooding events are not without ecosystem consequences. These climatic disturbances can result in more frequent germination of woody plants that require a threshold of moisture to germinate as seen in South Africa (Ward et al., 2014 and references within).

1.2 WOODY PLANT ENCROACHMENT

Woody plant encroachment is the process by which shrubs or trees grow with increasing frequency in areas that were historically grasslands or savannahs in response to a disturbance. In this circumstance, the woody vegetation is generally native to the region, but expand coverage at an accelerated rate in response to altered competitive dynamics (Burkhardt & Tisdale, 1976). Woody plant encroachment is often the result of overgrazing, fire suppression, climate or meteorological shifts, or a reduction in competition (Auken, 2000 and references within). The tropics and subtropics of the world have or are currently experiencing woody plant encroachment from grasslands and savannahs to forests due to reasons such as reduced frequency of fires and poor grazing practices (Archer, 1988; Asner, 2004; Auken, 2000; Sankey & Germino, 2008). Encroachment of mesic grasslands in The Great Plains has led to increases in infiltration but decreases in streamflow therefore reducing surface water availability (Zou et al., 2014). Increases in woody vegetation also lead to increases in rainfall interception and therefore direct evaporation. Intercepted water never becomes accessible to vegetation further limiting water supply and decreasing the amount of water that can infiltrate the ground and become recharge or storage (Honda &

Durigan, 2016; M. Keith Owens et al., 2006; Thurow et al., 2018). Ultimately, such changes in landcover will not only alter the evaporation and transpiration of a region, but will affect the potential for precipitation in downwind regions (Keys et al., 2014). For example, the Mau Forest in Kenya was clear cut and the following wet season experienced almost no precipitation because of the removal of trees (Hesslerová and Pokorný, 2010).

1.3 *JUNIPERUS ASHEI* ENCROACHMENT IN CENTRAL TEXAS

A classic example of woody shrub encroachment into a historic grassland is that of *Juniperus ashei* on the Edwards Plateau in central Texas. In the past 200 years, the density and range of *J. ashei* has increased, and is estimated to have increased by 35% in The Great Plains from 1949-1983 (Jessup et al., 2003; Miller and Rose 1995). Around the same timeframe live oak extended the range which it was found but not in the magnitude that juniper did (Smeins and Merrill, 1988). The Edwards Plateau is made up of mostly flat, thick layers of Cretaceous age limestone which erodes to form valleys over long timeframes (Hill & Vaughan 1898). Agriculture has long been present in the southeastern portion of the Edwards plateau in counties such as Blanco, Gillespie, and Comal; however, terrain in the western portion of the Edwards Plateau, known as the Hill Country, is not well suited for agriculture (Hill & Vaughan, 1898). An account from Bray (1904) describes the Hill Country as timbered in the lower, eroded portions and a grassland on the level uplands. Hill Country terrain is characterized by rocky hills with thin soil supporting short and mid-height grasses such as buffalo grass (*Buchloe dactyloides*), Texas cupgrass (*Eriochloa sericea*), and curly mesquite (*Hilaria belangeri*), sideoats grama (*Bouteloua curtipendula*), blue grama (*Bouteloua gracilis*) Texas grama (*Bouteloua rigidiseta*), and tridens pilosus (*Erioneuron pilosum*) among others (Riskind & Diamond. 1988). Forested areas are populated by plateau live oak (*Quercus fusiformis*), lacey oak (*Quercus laceyi*),

mesquite (*Prosopis* spp.), and ashe juniper (*Juniperus ashei*), which are also scattered throughout the upland savannahs (Riskind & Diamond, 1988). The prevalent native grasses led to a rapid expansion of the ranching industry and commensurate increase in the number of cattle brought to the area to graze in the early 1900's (Wilcox et al., 2012). Overgrazing of these grasslands by cattle, deer, sheep, and goats has ultimately led to soil depletion, compaction, erosion, and altering plant composition (Carlson & Glasrud, 2014; Eldridge et al., 2017). Deer often target oak seedling and saplings for food but are less likely to consume juniper. This sort of preferential foraging hinders oak establishment while increasing the number of junipers that reach maturity (Russell & Fowler, 2004).

The establishment of pastures throughout the Hill Country led to fire suppression efforts to protect homes and ranches. The suppression of the fire regime gave further advantage to juniper and facilitated competition with the fire-tolerant oaks (Abrams, 1992). Oak species in the region are more likely to recover after fire than junipers due to their ability to resprout after sustaining damage to leaves and crowns (Bryant et al., 1983; Reemts & Hansen, 2008). Wildfires reduce juniper populations and promote vegetation diversity by creating canopy gaps and reducing competition for limited water and nutrients (Yao et al., 2012). Fuhlendorf et al. (1996) developed a semiempirical statistical model to determine fire sensitivity of ashe juniper based life stages. Simulations were run on yearly timesteps and were based on a set of difference equations and probabilities of seedling establishment and mortality, from previous field studies. The results suggest that a cool season fire recurrence interval less than 25 years is necessary in order to maintain herbaceous cover and grassland biomass sufficient to prevent a closed canopy juniper woodland in the region (Fuhlendorf et al., 1996). In the absence of fire, juniper cover increases exponentially while herbaceous cover rapidly decreases becoming a closed canopy juniper forest in 75 years (Fuhlendorf et al., 1996).

1.4 JUNIPER CLEARING FROM THE TEXAS LANDSCAPE

Throughout the history of Texas, juniper was cleared for use as building material and for the expansion of cattle ranching (Bray, 1904). One method that was used is prescribed fires. A problem with using prescribed fires to remove juniper stands in the Edwards Plateau is the lack of understory shrubs and grasses to be used as fine fuel, without this fuel creating fires of high enough intensity and capability to become crown fires is much more difficult resulting in an inefficient method to remove juniper trees (Aro, 1983).

More recently, it has become common practice to remove juniper with the intent of water conservation (State Water Enhancement Plan, 2017). In 2011, The Texas State Soil & Water Conservation Boards created the State Water Enhancement Plan to emphasize water conservation and in it promoted the removal of brush species, notably *juniperus* species, in an effort to rejuvenate surface and ground water supplies (State Water Enhancement Plan, 2017). This plan is rooted in results from one report containing mixed results about the effects of brush control from the Research & Planning Consultants, and Espey, Padden Consultants Inc. (2000). Frequently studies of the effects of Juniper removal yield inconsistent results regarding increases in surface water and groundwater recharge. For example, a study done by Wong & Banner (2010) measured cave water drip rates pre- and post-clearing to determine changes recharge patterns and changes in the ratio of strontium isotopes in a cave due to a juniper clearing. Drip rates provided inconclusive results on the effect of juniper removal on groundwater recharge and residence time due to high variability of precipitation patterns throughout the study while strontium isotopes indicated no change in residence time. The combination of methods used assist with interpretation helping to eliminate anomalies from factors such as higher precipitation. Results from Wilcox et al. (2005) indicated no change in streamflow after clearings on 6 first order watersheds. The streams that were monitored were intermittent streams and only

flowed for short periods of time following precipitation. The study concluded that streams more likely to benefit from woody plant removal are those that exhibit continuous baseflow. A few studies have seen positive results with juniper clearing. Increases in streamflow of 46 mm year^{-1} were observed by Huang and Wilcox (2006) after partial clearing of juniper in a first order watershed. Likewise, a study by Dugas (1998) showed a temporarily increased water yield for two years after clearing and a decrease in evapotranspiration by 0.3 mm day^{-1} . Perhaps the best-known example of juniper clearing for water conservation is that of Selah Ranch in Blanco, Texas. In 1969, more than 3000 acres of juniper were cleared and native grasses re-sown. Two and a half years after the juniper clearing, a new spring appeared on the property. The owner attributes its appearance to the establishment of the grasses and its ability to slow runoff and promote infiltration into a perched water table. In the subsequent years ten springs appeared along with two streams (Pasztor a, 2020). However, land cover change was not the only modification made to the Selah landscape. Large berms were constructed horizontally along slopes to slow the flow of runoff, which has also been hypothesized to increase recharge (Pasztor b., 2020).

Changes in vegetation cover have significant impacts on the surface water budget, resulting in potential increase in water availability leading to overall changes in transpiration rates. Previous studies have shown that direct measurements of tree sap flow are very useful to examine the effect of changes in land cover on stand water balance (Chemura et al., 2020; Macfarlane et al., 2010; Moore et al., 2004). Having information on the amount of water used by each species by gathering sap flux data pre- and postclearing will help give insight on the effects and potential benefits of juniper removal. In the present study, we endeavor to elucidate transpiration rates in three hill country tree species in response to a partial clearing of juniper within a first order watershed in Edwards County,

Texas. Data was collected for one year prior to juniper removal (2018) and compared to data collected post removal (2019). The goals of this study were to: (1) determine typical transpiration rates of the dominant native tree species, (2) determine whether elevation or location along a hillslope played a role in water availability to roots, and (3) compare transpiration rates before and after clearing to determine if water availability increased.

Chapter 2: Methods

2.1 FIELD SITE DESCRIPTION

The study was conducted on a privately-owned ranch on the Edwards Plateau 31 kilometers SW from the town of Rocksprings, Texas (Latitude 29.885519° Longitude - 100.495890°) at an elevation of 660 meters. The annual average temperature is 21.1°C with a mean annual rainfall of 158 mm during the peak growing season which we define here as day of year (DOY) 120-300. While conditions are favorable for a nearly continuous growing season for many species at the site, we selected DOY 120-300 as peak growing season to encapsulate only the period when both evergreen and deciduous tree species were fully leafed out. The site consists of two main soil types: the Oplin-Rock outcrop complex which hits bedrock at 38 cm depth, and the Eckrant-Rock outcrop complex which becomes bedrock at 30 cm depth (Soil Survey Staff, 2017). The parent material and bedrock is limestone (Soil Survey Staff, 2017). The dominant tree species at the site are lacey oak (*Quercus laceyi*), escarpment live oak (*Quercus fusiformis*), Texas pinyon pine (*Pinus remota*), and ashe juniper (*Juniperus ashei*). The understory is primarily composed of Texas persimmon (*Diospyros texana*), agarita (*Mahonia trifoliolata*), prickly pear (*Opuntia lindheimeri*), and sparse native grasses. During the period between March 25th (DOY 84), 2019, and mid-April 2019 (DOY 106), 25 acres of *J. ashei* were cleared from upslope areas of the property, and a mix of native grasses and wildflowers were seeded in cleared areas (Figure 1).

We measured local micrometeorological conditions and sap flux, as a proxy for transpiration, from DOY 120, 2018 until DOY 300, 2019. This timeframe was chosen to maintain a consistent interval between years encompassing the growing season, to ensure all species had leafed out, and because the site was not established until DOY 120 in 2018.

A total of 16 sap flux sensors were installed in three canopy-dominant tree species of varying sizes to create a representative distribution of the rate and volume of transpiration from the forested area (Figure 1). The height, tree crown, and diameter at breast height (DBH, cm) were measured for each of the sensed trees to insure size a representative size distribution. Volume of transpiration for hypopthesis (1) and (3) was determined using sap flux data and active sapwood area which was determined by collecting cores from a large range tree sizes to determine the allometric relationship between sapwood and DBH. Leaf water potentials and diurnal sap flux curves were measured to investigate hypothesis (2) a potential relationship between elevation and water availability.

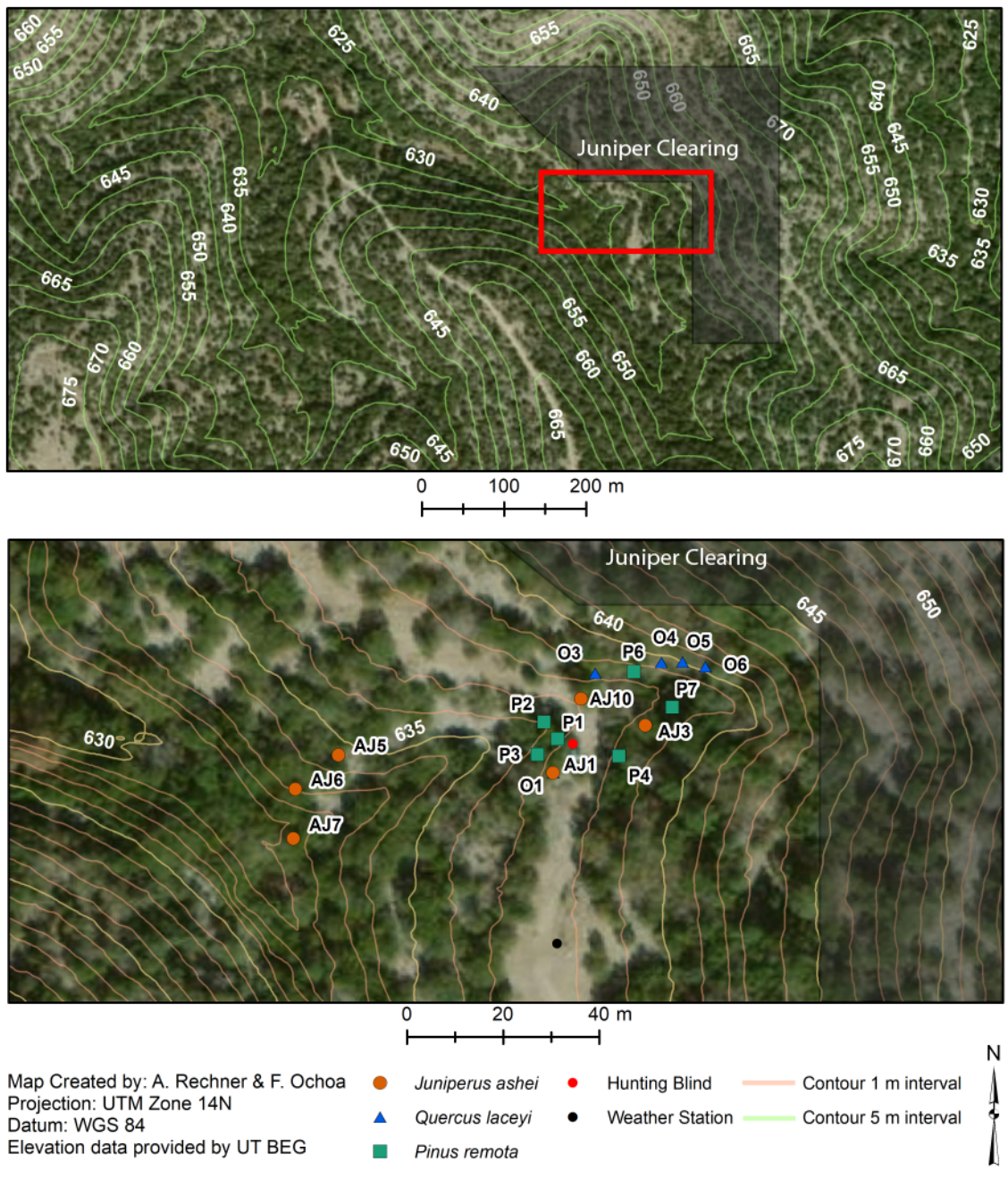


Figure 1: The contour map on the top is an extended view of the surrounding topography with 5-meter contours. The red box within the top image is the sap flux site. The bottom image shows the locations of the different oaks (blue triangles), pines (green squares), junipers (orange circles) with sap flux sensors installed with 1-meter contours. The gray shadow in the top right is the area where the clearing happened in the spring of 2019. Table 2 shows the descriptions of the trees labeled in this figure.

2.2 SAP FLUX

2.2.1 Sensor Theory

Sap flux measurements provide the closest approximation for transpiration at the individual tree scale. This method is based on the assumption that the heat input by the sensor under steady sap flow conditions is equal to the heat dissipation (via convection and conduction) along the interface between the sensor and the tree when the sensor and the tree are in thermal equilibrium. Daily fluctuations in the heat dissipated from the sensor are compared to the unheated temperature of the tree sap and wood (Davis et al., 2012). The sap flux sensors (Figure 2) used for this study were hand-constructed following the original thermal dissipation sensor design of Granier (1987). Each sensor consists of two thermocouple-containing needles, aligned 10 cm vertically apart, and inserted into the trees' hydro active xylem. The needle on top is wound in a constantan wire which is supplied with a constant current to generate heat. The thermocouple located in the bottom needle measures the reference temperature of the sap while the thermocouple in the top needle measures the amount of heat being dissipated by the vertical motion of the sap.

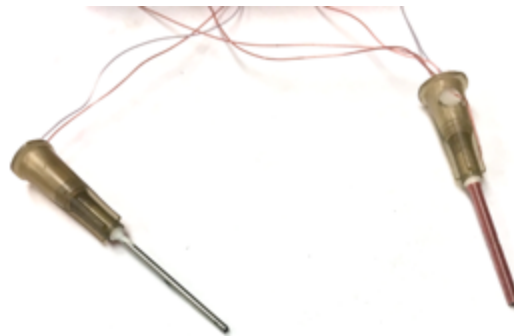


Figure 2: Example of a hand-made thermal dissipation probe sap flux sensor with the heating wire located on the right needle.

If sap is not flowing, the temperatures of the two thermocouples are similar. As the tree transpires and sap flows vertically upward through the conductive tissue, it carries the

heat with it creating a temperature difference between the two thermocouples. This temperature difference, measured in millivolts, is ultimately used to calculate sap flow velocity.

2.2.2 Sensor Construction

The sensors are made from 19-gauge hypodermic needles (Becton Dickinson, Franklin Lakes, NJ, USA) that have been cut to 2 centimeters using a Dremel tool. The cut needles are polished to eliminate rough/sharp edges. A hole is cut partially through the metal needle body, 1 cm from the tip of the needle. This hole or ‘viewing window’ is used for thermocouple placement. For the heating needle, a 0.125 diameter hole is also made in the plastic base in order to secure the heating wire in place. A pair of needles is then connected via a 30 cm constantan wire (Item TFCC-005-100, Omega Engineering, Stamford, CT, USA) with a diameter of 0.127 mm. Each needle is then threaded with a copper wire (Item TFCP-005-100, Omega Engineering, Stamford, CT, USA) with a diameter of 0.125 mm and length of 15 cm. One end of each copper wire is connected to the respective end of the 30 cm constantan wire to form a thermocouple inside of each needle. Finally, a second constantan wire (50 cm) is threaded through the heating needle until the end coming out of the plastic base is even with the other wires. The thermocouples are slid into the needles by gently pulling the wires from the plastic base until the thermocouple connection can be seen in the viewing window in the middle of the needle. Thermocouples are glued in place in the viewing window using a flexible, rubberized adhesive (Loctite 308 Black Max, Henkel, Dusseldorf, Germany). The adhesive is allowed to cure for a week. After curing, the remaining tips of insulation are removed for an approximate length of 0.5 cm. At this stage, quality control is enforced by verifying that the resistance for each wire/connection is within the acceptable range (Table 1). Starting at

the needle tip and working towards the plastic base the 50 cm constantan wire is tightly wound around the needle such that the coil does not move and no gaps are present. At the base of the needle, the constantan heating wire is pulled through the hole in the plastic base (Figure 2). The plastic bases of both needles are then filled with white craft glue to secure the wires and prevent unwrapping of the heating wire. Sensors are suspended upside down for 24 hours to allow the glue to dry. The resistance of the sensors is tested again after the glue has dried to verify secure connections and proper functionality (Table 1).

Table 1: Acceptable resistance ranges for wired connections during sap flux sensor assembly.

Wires	Connection	Resistance (Ω)
Constantan - Constantan	Heating wire to self	22-24
Copper - Copper	Thermocouple to Thermocouple	14-16
Constantan - Copper	Heating wire to either Thermocouple	Infinite/no connection

2.3 FIELD SITE SETUP

Sap flux data were logged using a CR1000x datalogger (Campbell Scientific) installed in a weatherproof enclosure mounted beneath a hunting stand. Continuous 12V power was supplied to the logger from a solar array on the roof of the hunting stand. Sap flux measurement trees were selected to be representative of the relative distribution of species and sizes throughout the research plot based on the DBH. Six *J. ashei*, five *Q. laceyi*, and five *P. remota* spanning the diameter of 8.2-36.4 cm were instrumented (Table 2). Instrumented trees were placed into the following size classes medium trees ($13 \text{ cm} \leq \text{DBH} \leq 24 \text{ cm}$) and large trees ($\text{DBH} > 24 \text{ cm}$).

Table 2: Data related to trees with sap flux sensors.

Tree	DBH (cm)	Height (m)	Tree Crown Area (m ²)	Sap Wood Area (cm ²)
Pinyon 1	18.4	6.4	12.7	157.7
Pinyon 2	14.8	7.0	19.6	112.2
Pinyon 4	30.8	13.4	59.5	314.3
Pinyon 6	19.1	10.9	25.1	166.5
Pinyon 7	25.5	11.8	52.4	247.3
Oak 1	14.4	11.9	34.4	75.5
Oak 3	15.0	8.7	10.2	83.9
Oak 4	19.9	21.9	48.9	151.9
Oak 5	31.7	13.9	73.3	315.7
Oak 6	24.0	15.9	79.9	208.8
Juniper 1	27.3	8.1	46.1	545.5
Juniper 3	31.4	11.0	46.2	547.1
Juniper 5	18.8	10.5	17.4	126.9
Juniper 6	36.4	15.9	37.9	426.7
Juniper 7	24.3	11.6	30.8	322.1
Juniper 10	22.9	10.6	27.3	272.0

2.3.1 Sap Flux Sensor Installation

Sap flux sensors are installed by first removing the bark to the cambium on the north face of the tree using a draw knife. Two holes are pre-drilled 10 cm apart vertically at breast height (1.37m) using a 3/32-inch bit. A 20 mm length of 14-gauge aluminum hypodermic tubing (Grainger Industrial, Lake Forest, IL, USA) is inserted into each hole to assure uniform heating and provide protection to the sensor from trunk growth. Sensors are greased with conductive thermal paste (ThermalCote 250G, Aavid Thermolly,

Concord, NH, USA) to promote even heat dissipation and inserted into the 14-gauge tubes (Figure 3).



Figure 3: Sap flux sensor installation. Top needle has the heating coil, and the bottom measures the reference temperature.

Sap flux sensor wires are connected via soldered connection to a CAT-5 cable (CAT-5E, Priority Wires and Cables, INC, Little Rock, AR, USA). The CAT-5 cables connect trees to the central enclosure box where the data logger is housed. In the enclosure box, CAT5 wires connect to circuit boards which supply continuous 0.2W of heating power and to the multiplexor from which data is transmitted to the datalogger. The voltage difference from each thermocouple pair is measured and recorded every minute and averaged to hourly timesteps. Finally, sensors are covered by a piece of reflective insulation (Reflectix Radiant Barrier, Reflectix Inc, Markelville, IN, USA) to provide protection from solar heating and environmental threats (Figure 4).



Figure 4: Sap flux sensors installed and covered by reflective thermal insulation.

2.4 TREE CORES

Tree cores were used to access sapwood area which is used to convert sap flux to transpiration. We cored a broad size range of trees for each species to determine allometric relationships between sapwood area and DBH (Figure 5). Cores were extracted at breast height using an increment borer. Sapwood depth was determined through visual estimation of each core and converted to sapwood area assuming sapwood forms an annulus (Equation 1) around the tree. For cores where visual estimation was difficult or inconclusive, we verified field estimations in the lab using a dissecting light microscope.

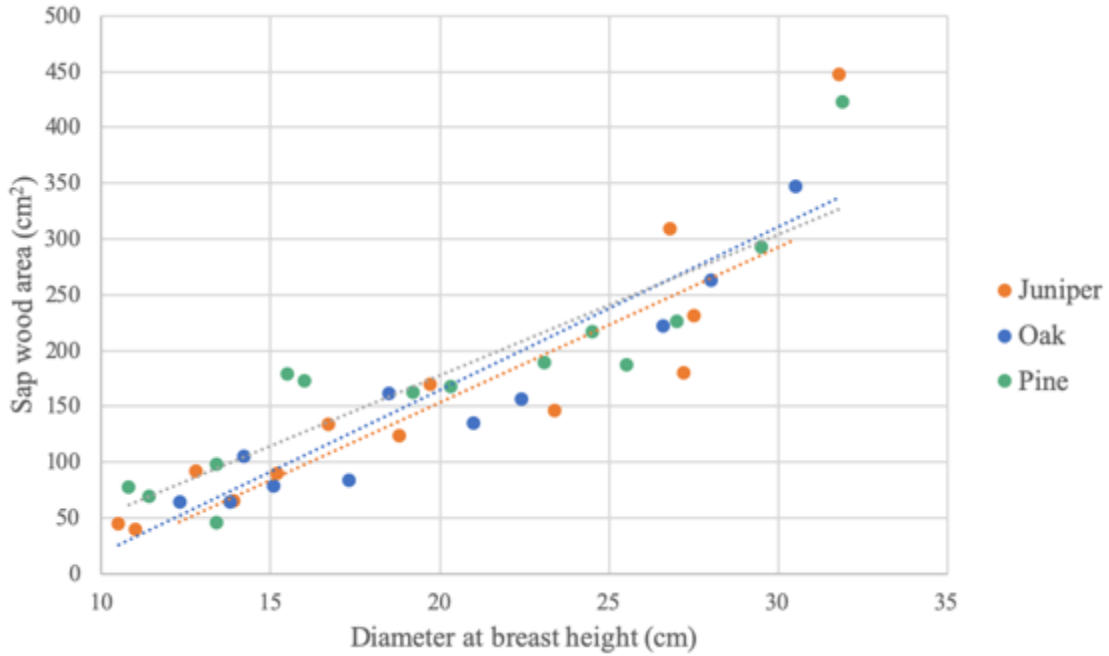


Figure 5: Sapwood area is linearly related to diameter at breast height (DBH) for all three species. The dotted lines are lines of best fit.

Table 3: Equations for the line of best fit for each species from Figure 6.

Species	Equation of Fit Line	R ²
Juniper	$y = 14.60 x - 127.17$	0.80
Oak	$y = 13.88 x - 124.31$	0.90
Pine	$y = 12.63 x - 74.71$	0.81

The area of the annulus of sapwood (A_0 , cm²) was calculated using Equation 1 and was plotted with DBH in Figure 5 above.

$$A_0 = \pi(R^2 - r^2) \quad (1)$$

We used these allometric relationships (Table 3) to approximate the sapwood area for each instrumented tree (Table 2).

2.5 TREE CROWN AREA AND HEIGHTS

Tree crown area and height were measured along with DBH to identify trees that would give a representative sample of the surrounding woodland. The tree crown area for

each tree with a sap flow sensor installed was measured (Table 2). Tree crown area was calculated by measuring the perpendicular major and minor axis of the crown with the assumption that the crowns are elliptical. The extents of major and minor axes were approximated from the ground and lengths were measured via survey tape. The tree height (h , m) was calculated using a digital protractor. A spotter walked and measure a distance (d , m) from the tree at which the top of the crown is visible. The spotter then lined the top of the tree crown with the crosshair of the digital protractor and recorded the angle (θ , degrees). The eye level height of the spotter (y , cm) was measured using a measuring tape. The height of the tree was calculated following Equation 2.

$$h = d \tan(\theta) + y \quad (2)$$

2.6 LEAF WATER POTENTIALS

We use leaf water potential measurements to determine the plant water status and hydraulic strategies. Leaf water potential measurements were performed using pressure chambers (PMS Model 600 and 600D, Albany, OR, USA) at pre-dawn (6:00), midday (12:00), early evening (16:00), and late evening (18:00). Leaves or, for needle-leaf species, clusters of leaves, receiving full sun were removed from the tree by hand or pole-pruner. Petioles were recut with a razor blade and threaded through the gasket and sealed into the chamber. The rate valve was adjusted to increase the pressure inside of the chamber via nitrogen addition until water first appeared on the cut end of the petiole. At this moment, the pressure was recorded. The measurements were performed in triplicate and averaged for each tree at each time of day. The trees used for these measurements were juniper 7, juniper 10, pine 6, oak 8. Measurements started on DOY 32 (February 1st, 2020) at noon and ended after predawn measurements on DOY 34 (February 3rd, 2020). Measurements resumed on DOY 66 (March 6th, 2020) at 16:00 and ended after the collection of noon

measurements on DOY 68 (March 8th, 2020). This gave a total of four triplicate measurements for each tree.

2.7 HYDRO-METEOROLOGICAL MONITORING STATION

A micrometeorological station was installed adjacent to the sap flux measurement plot (Figure 1). We measured ambient air temperature, relative humidity (EE181-L10-PT, Logan, UT, USA), and air pressure (CS100, Logan, UT, USA). Soil moisture (or soil water content, SWC) was measured at 10 cm depth at which point bedrock was blocking deeper installation (CS655-17-PT-DS, Logan, UT, USA). We measured broad-spectrum shortwave radiation (CS320-T5, Logan, UT, USA) and solar radiation (LI190R-L15-PT, Logan, UT, USA). Precipitation was measured using a tipping bucket system (TE525WS-L25-PT, Logan, UT, USA). Leaf wetness, or water accumulation on the leaves, was recorded (LWS-L15-PT, Logan, UT, USA). We also measured wind speed and direction (Windsonic1-L14-PT, Logan, UT, USA). All data was recorded at 5-minute intervals, and stored in hourly time steps (CR6, Campbell Scientific, Logan, UT, USA).

2.8 DATA PROCESSING

2.8.1 Hydro-meteorological Data Processing

Hydro-meteorological data was recorded every 5 minutes, averaged into half hourly intervals, and concatenated into annual files. Vapor pressure deficit (VPD, kPa) is how much water vapor the air is holding versus how much water the air holds when saturated (Lambers, Chapin, & Pons, 2009). VPD was calculated in half hour averages by taking the difference of the saturation vapor pressure ($e_{saturated}$, kPa) (Equation 3) and ambient vapor pressure (e , kPa) (Equation 4) included in the meteorological data. The saturation

vapor pressure is the amount of water vapor to reach the point of saturation and was calculated using Equation 3.

$$e_{saturated} = .611e^{\frac{17.502*T}{T+240.97}} \quad (3)$$

The ambient vapor pressure was calculated using Equation 4.

$$e = \left(\frac{RH}{100}\right) * e_{saturated} \quad (4)$$

VPD was calculated using Equation 5.

$$VPD = (e_{saturated} - e) \quad (5)$$

2.8.2

Raw sap flux data (mV) was converted into sap flux density ($\text{gH}_2\text{O s}^{-1}\text{m}^{-2}_{\text{sapwood}}$) using the methods originally developed by Granier (1987) ($K = \Delta T_{max} / \Delta T_{sensor} - 1$

$$F_s = K * u * S_A \quad (7, \text{ and Equation } F =$$

$\int_a^b u * S_A * dt$ (8). To account for differences between individual hand-manufactured sensors and sensor drift, we employed a nocturnal baseline procedure developed by Oishi (2008, 2016). Through this procedure, each sensor is calibrated to itself nightly. We define the maximum temperature difference (ΔT_{max} , mV) for each sensor as representative of no-flow conditions. In order to establish these baseline points (ΔT_{max}), a no-flow must occur at night and when VPD is below a threshold value (Oishi et al., 2016). The Oishi baseliner sets the baseline points when VPD has a two-hour average less than 0.05 kPa and when the standard deviation of the four highest ΔT values are less than 0.5% of the average of these four values. These conditions may not occur every night which gives this method the ability to account for the potential of nocturnal flow (Oishi et al., 2008). Once the ΔT_{max} points were determined, a linearly interpolated baseline for ΔT_{max} was calculated. ΔT_{max} was then paired with the half hourly temperature difference data from each specific sensor ΔT_{sensor} to calculate K , a dimensionless quantity.

$$K = \frac{\Delta T_{max}}{\Delta T_{sensor}} - 1 \quad (6)$$

From K the mean sap flux density (u , $\text{g}_{\text{H}_2\text{O}}\text{s}^{-1}\text{m}^{-2}_{\text{sapwood}}$) is calculated. This is the instantaneous amount (mass) of water passing through per square meter of sapwood. A one hour moving average was applied to u for all days in 2018 and 2019.

$$u = 119 * K^{1.123} \quad (7)$$

In this study, transpiration ($\text{kg}_{\text{H}_2\text{O}} \text{day}^{-1}$) is quantified as the total amount of water being lost to the atmosphere over a fixed period, e.g., a day. Daily transpiration is calculated by computing the integral of u multiplied by sapwood area (S_A , m^2) where b is time at the end of the day and a is the time at the beginning of the day.

$$F = \int_a^b u * S_A * dt \quad (8)$$

Chapter 3: Results

3.1 SITE METEOROLOGY AND INTERANNUAL VARIABILITY

The meteorological conditions during the growing season of 2018 and 2019 were similar with respect to temperature, VPD, and total precipitation (Table 4). Temperature increased by 1.6% from 2018 to 2019. Likewise, VPD increased by 4.4%, and precipitation increased by 2.5% from 2018 to 2019 (Table 4). The total amount of precipitation varied by < 3% between years, however, the frequency and distribution of storms were markedly different (Figure 6 and Figure 7). Precipitation was more frequent in 2018 than 2019; however, the average total rainfall per event was less than 5 mm (Figure 6). In 2019, there were more than six days with precipitation events greater than 5 mm, with most of the precipitation occurring between DOY 120 and 176 (Figure 7). From DOY 176, 2019, through DOY 300, 2019, the total precipitation was only 6.60 mm (Figure 7). The mean SWC in 2019 ($0.175 \text{ m}^3_{\text{H}_2\text{O}} \text{ m}^{-3}_{\text{soil}}$) decreased significantly by 29.3% compared to 2018, which is directly related to a decrease in the frequency and amount of precipitation events in 2019 (Table 4). The latter half of 2019 was classified by the Palmer Drought Severity Index (PDSI), using the National Oceanic and Atmospheric Administration data, as a drought year. The SWC remained below $0.15 \text{ (m}^3_{\text{H}_2\text{O}} \text{ m}^{-3}_{\text{soil}})$ in 2019 from DOY 196 through the end of the year (Figure 7).

Table 4: Mean hydro-meteorological parameters for DOY 120 - 300 for 2018 and 2019. Values in parenthesis are the standard deviations for the growing period selected. The third column is the percent change in averages between 2018 and 2019.

Hydro-meteorological Parameters			
	2018 (DOY 120-300)	2019 (DOY 120-300)	Percent Change (%)
Temperature (°C)	24.9 (±6.2)	25.4 (±5.9)	1.6
Total Precipitation (mm)	156	160	2.5
Vapor Pressure Deficit (kPa)	1.30 (±1.28)	1.36 (±1.13)	4.4
Soil Water Content (m³ H₂O m⁻³ soil)	0.248 (±0.14)	0.175 (±0.13)	-29.3
Relative Humidity (%)	68.3 (±23.1)	64.7 (±20.8)	-5.3

Pines showed a large increase in sap flux during the cooler, wet conditions that occurred near DOY 300-365; in 2018 sap flux values reached between 30-45 ($\text{g}_{\text{H}_2\text{O}}\text{s}^{-1}\text{m}^{-2}_{\text{sapwood}}$) (Figure 6D). The higher rate of sap flux for pine continued into 2019 until DOY 115 (Figure 7D). Juniper sap flux decreased in parallel with soil moisture starting at DOY 204, 2019, and remained at the lowest flux magnitudes of all species for the remainder of the year (Figure 7E). The pines and oaks continued to transpire during this period, but at a lower rate than earlier in the year (Figure 7D and E).

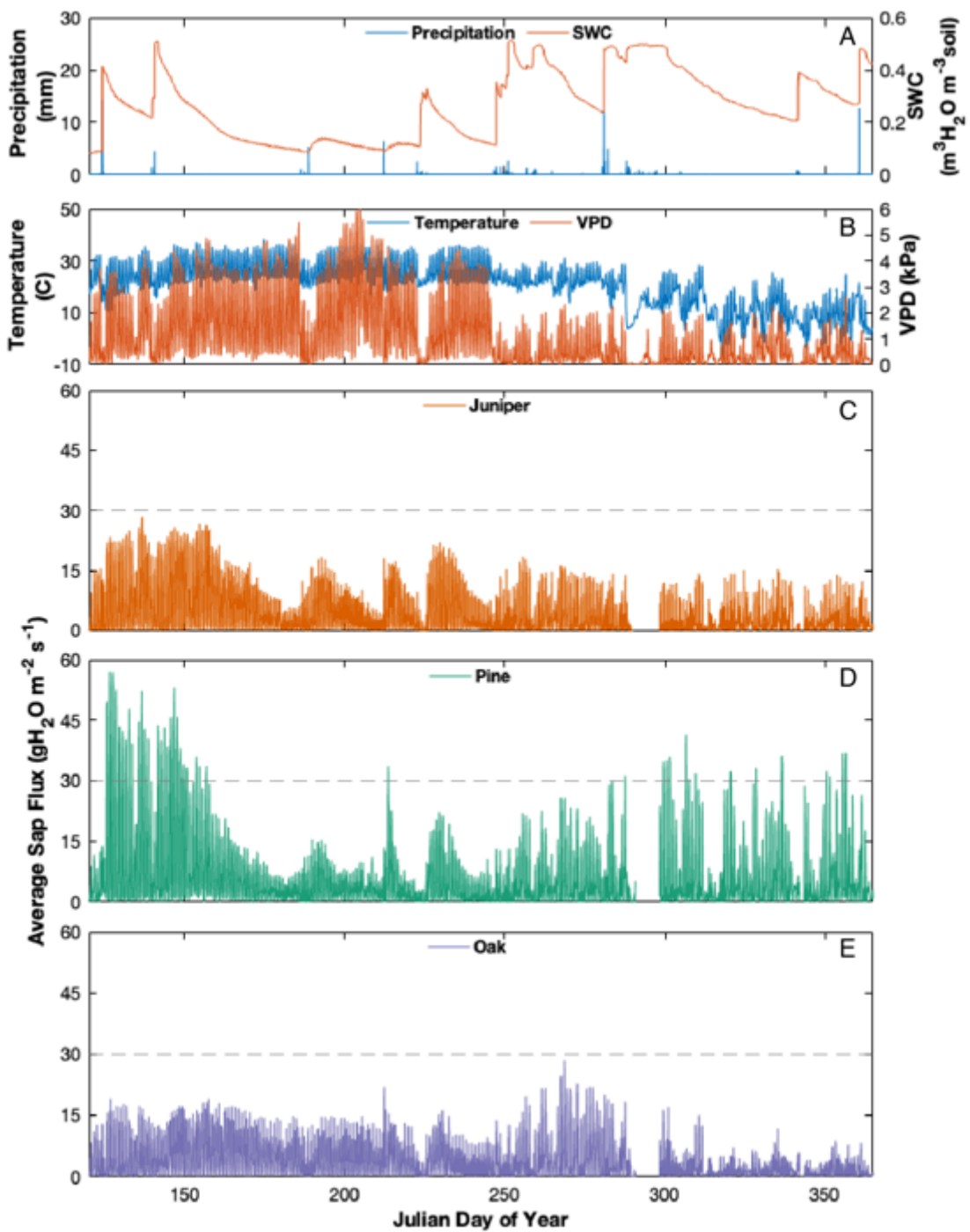


Figure 6: 2018 time series of hydro-meteorological and sap flux data at a half-hourly time step. The top plot shows a strong relationship between precipitation and SWC. The second plot (B) shows temperature and VPD. The bottom three plots (C, D, E) shows the average sap flux by species from DOY 120-365 with a gray dashed line for reference between species and years (Figure 7).

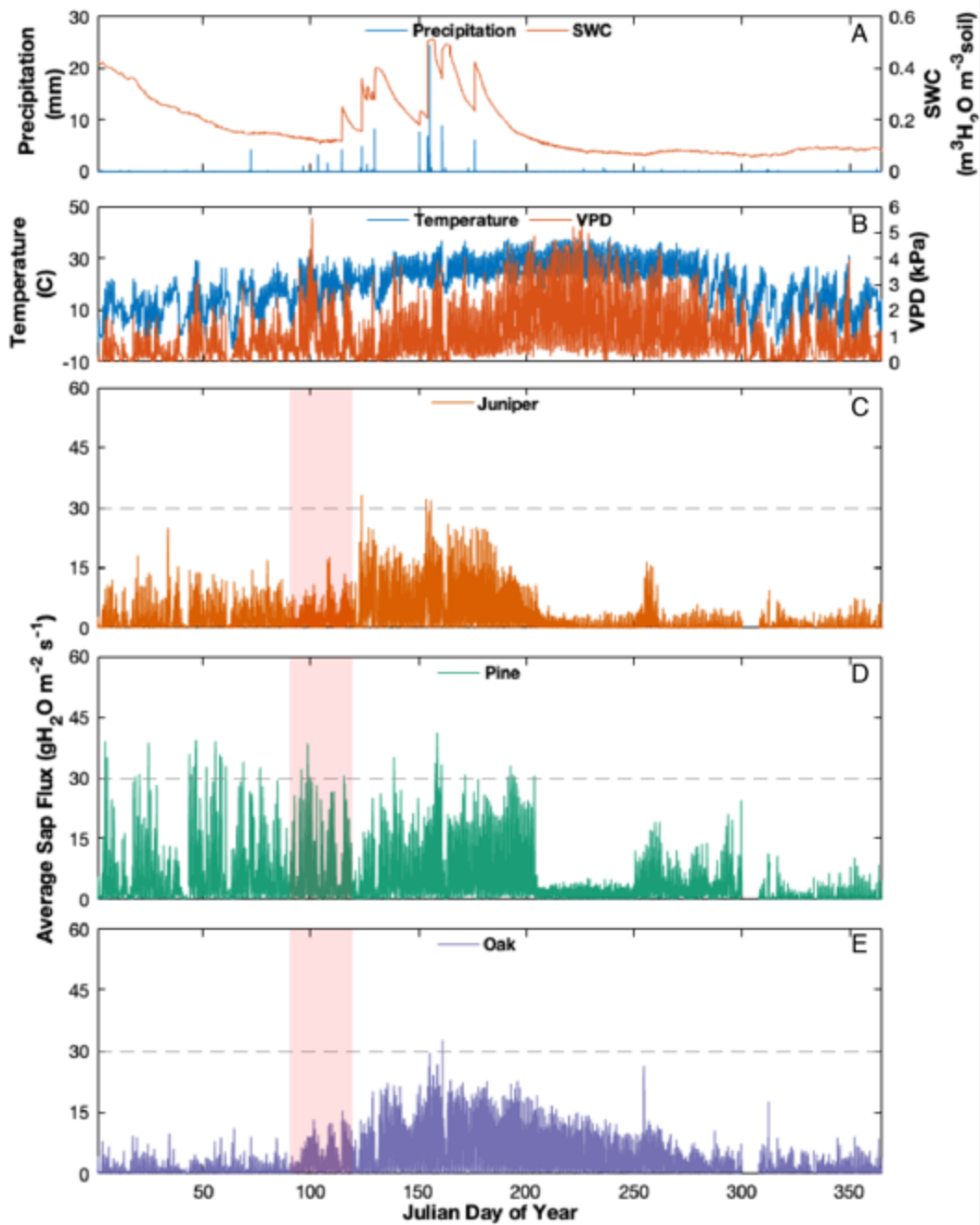


Figure 7: 2019 yearly time series of meteorological and sap flux data consisting of half hour averages. The bottom three plots (C, D, E) shows the average sap flux by species. The bottom plot shows the average sap flux by species. The red box over DOY 84-106, indicates the period of active removal of junipers, and the gray dashed line is for comparisons between species and years (Figure 6).

3.2 PRE- AND POST-CLEARING COMPARISONS

3.2.1 13-Day Similar Hydro-meteorological Conditions Comparison

In order to compare pre- and post-clearing transpiration rates, while minimizing the influence of interannual variability in hydro-meteorological conditions, we selected a thirteen-day period in each year with similar meteorological conditions and adequate soil moisture to promote transpiration (Table 5). Precipitation occurred three days prior to each of these periods on DOY 139 and 140 in 2018 totaling 5.9 (mm), and DOY 176 in 2019 totaling 6.1 (mm).

Table 5: Comparison of hydro-meteorological conditions for a 13-day period representing preclearing (2018) and post clearing (2019). The two periods are within ~20% of each other in terms of all parameters below.

Hydro-meteorological Parameters			
	2018, DOY 143-155	2019, DOY 179-191	Percent Change (%)
Temperature (°C)	27.5 (±4.7)	27.0 (±4.1)	-1.8
Total Precipitation (mm)	0	0	0.0
Vapor Pressure Deficit (kPa)	1.69 (±1.17)	1.34 (±1.00)	-20.9
Soil Water Content (m³H₂O m⁻³soil)	0.305 (±0.059)	0.251 (±0.048)	-17.8
Relative Humidity (%)	60.3 (±18.8)	62.0 (±17.3)	2.6

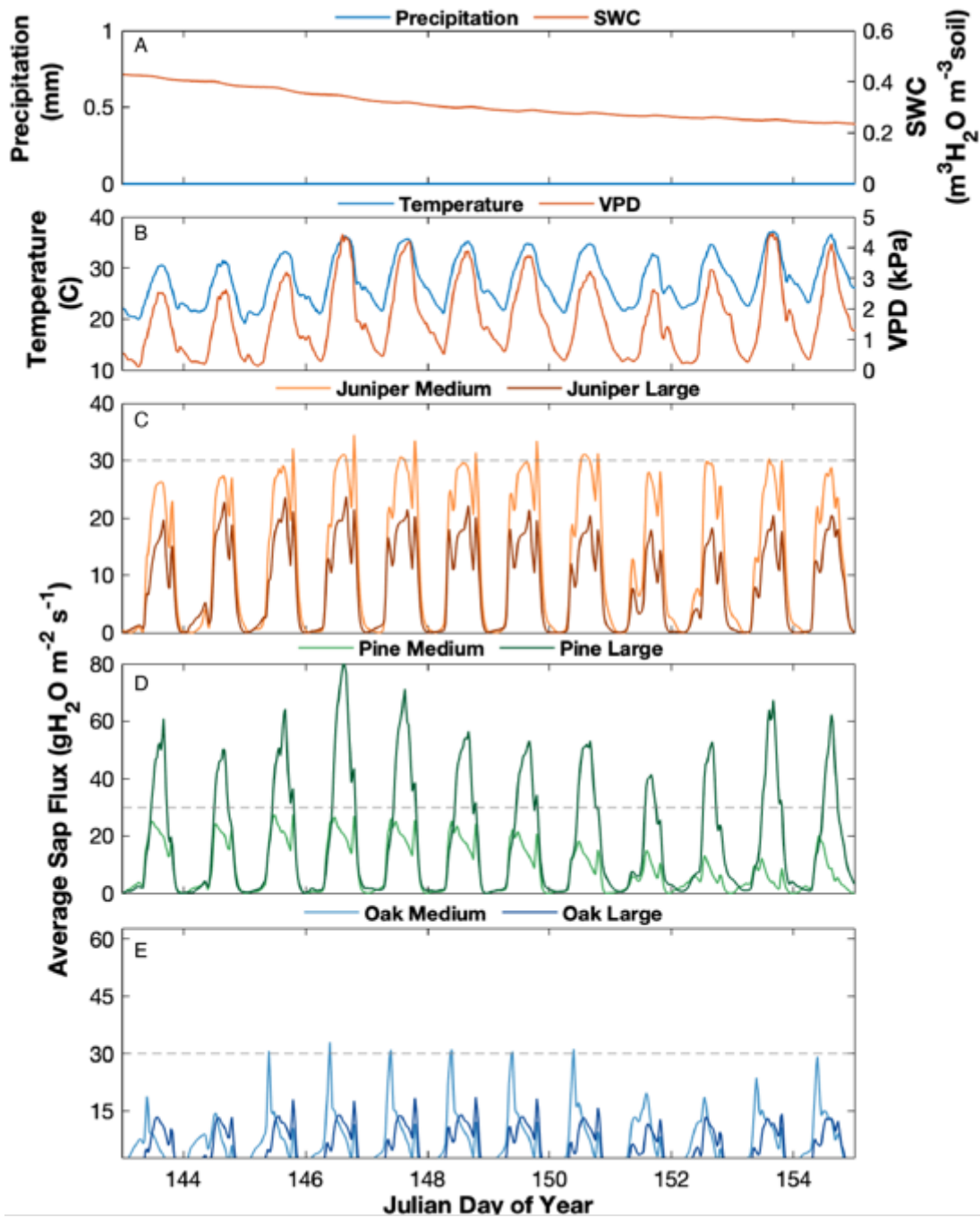


Figure 8: 2018, 13-day period before juniper clearing with soil conditions continuously getting drier (A). The bottom three plots (C, D, and E) show sap flux for each species by medium ($13 \text{ cm} \leq \text{DBH} \leq 24 \text{ cm}$) and large ($\text{DBH} > 24 \text{ cm}$) size classifications. The gray dashed line (C, D, and E) is a reference to compare between species and year (Figure 9).

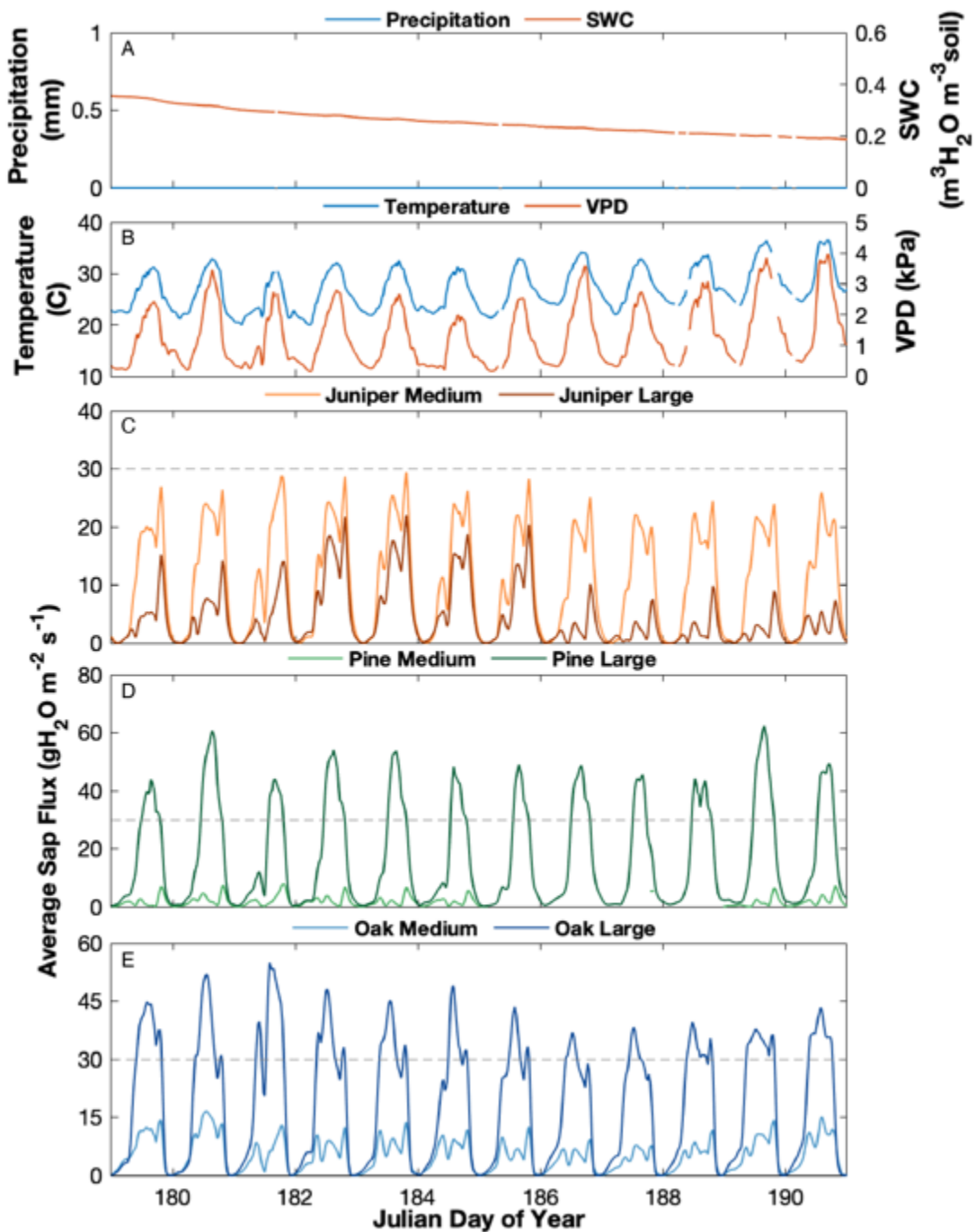


Figure 9: 2019, 13-day period post juniper clearing with soil conditions continuously getting drier (A). The bottom three plots (C, D, and E) show sap flux for each species by medium ($13 \text{ cm} \leq \text{DBH} \leq 24 \text{ cm}$) and large ($\text{DBH} > 24 \text{ cm}$) size classifications. The gray dashed line (C, D, and E) is a reference to compare between species and year (Figure 8).

Juniper trees of both size medium ($13 \text{ cm} \leq \text{DBH} \leq 24 \text{ cm}$) and large ($\text{DBH} > 24 \text{ cm}$) classes reduced sap flux in response to declining soil water content beginning on DOY 186, 2019, when SWC equaled $0.23 \text{ m}^3_{\text{H}_2\text{O}} \text{ m}^{-3}_{\text{soil}}$ (Figure 9C). In 2018, the midday peak sap flux for medium pines was near $20 \text{ g}_{\text{H}_2\text{O}}\text{m}^{-2}_{\text{sapwood}}\text{s}^{-1}$ for the first eight days and dropped by $\sim 10 \text{ g}_{\text{H}_2\text{O}}\text{m}^{-2}_{\text{sapwood}}\text{s}^{-1}$ for the remaining days as soil moisture declined (Figure 8D). Oaks registered only minor declines in peak daily sap flux with decreases in SWC (Figure 8D, Figure 9D). For these two comparison periods, the only increase in transpiration was evident in large oaks (105%). However, when analyzed over the entire growing period (DOY 120 - 300) all species increased transpiration from 2018 to 2019, in spite of the extreme soil drought in late 2019. On a per species average, oaks experienced an increase in sap flux by 45.5% while pines and junipers decreased by 19.8% and 17.9%, respectively during this comparison period (Table 6).

Table 6: Comparison of transpiration rate for pre- and post-clearing 13-day period.

Transpiration Rate (kg day^{-1}) for 13- day period pre- and post-clearing			
	2018 (DOY 143 - 155) Pre-clearing	2019 (DOY 179 - 191) Post-clearing	Percent Change (%)
Juniper	19.2	15.7	-17.9
Pine	25.5	20.5	-19.8
Oak	11.0	16.0	45.5

3.2.2 Sap Flux Compared During Changing Soil Conditions

Mean daily sap flux values for each species were compared to mean daily SWC for 2018 (Figure 10A) and 2019 (Figure 10B). During 2018, oaks ($R^2 = 0.28$) and pines ($R^2 = 0.22$) which is considered a strong relationship between sap flux and SWC, when fit with

a logarithmic curve (Table 7) because of other factors that effect to sap flux such as VPD, cloud cover, temperature, and others. After the juniper clearing (DOY 106) in 2019, junipers ($R^2 = 0.37$), pines ($R^2 = 0.20$), and oaks ($R^2 = 0.67$) showed strong relationships between sap flux and soil water content (Table 7). For all species, the relationship between sap flux and soil water content were stronger in 2019 than 2018.

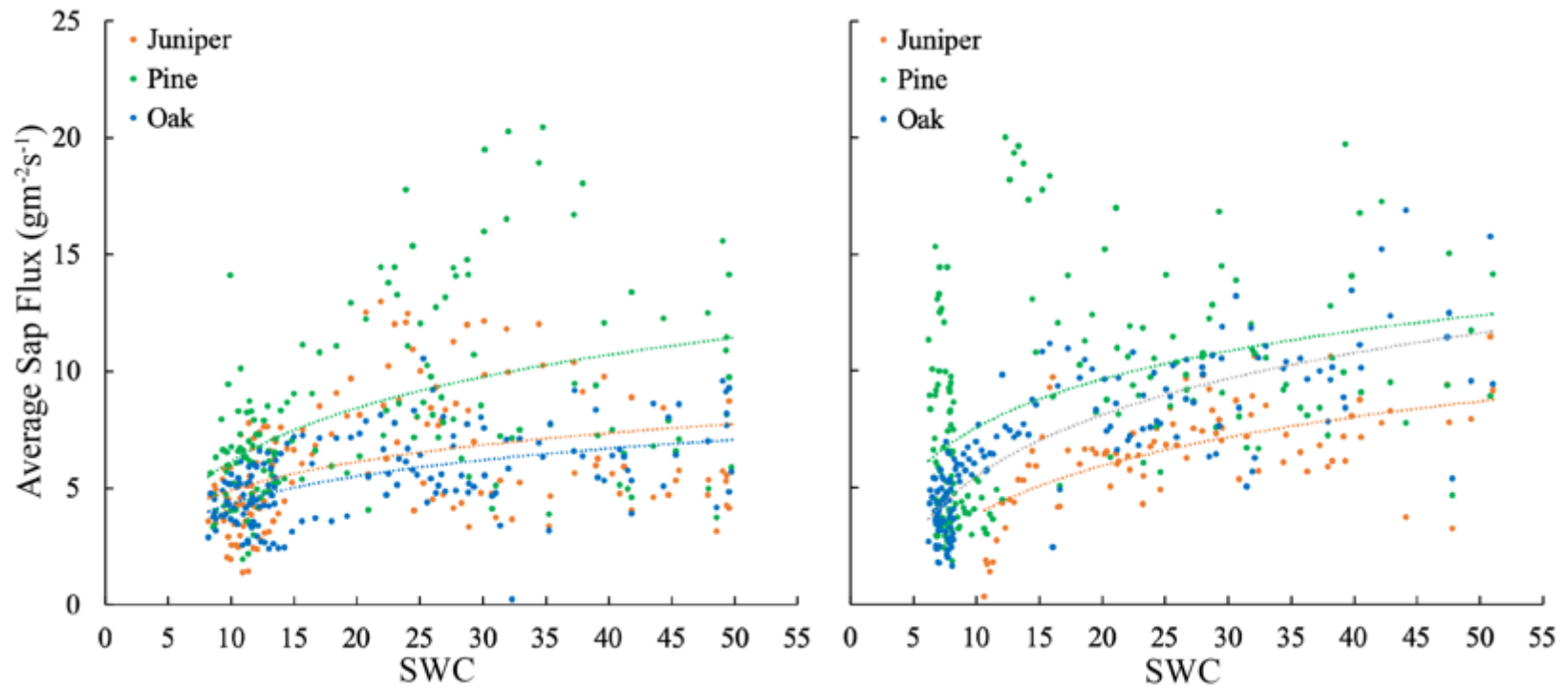


Figure 10: Average daily sap flux values compared with average daily SWC for DOY 120-300 in 2018 (A) and 2019 (B) for oak (blue), pine (green), and juniper (orange). The dotted lines represent the logarithmic line of best fit for each species.

Table 7: Equations of best fit and their R² values for 2018 and 2019 comparison of sap flux and SWC shown in Figure 11. The best fit is a logarithmic curve.

	2018		2019	
	R ²	Equation of fit	R ²	Equation of fit
Juniper	0.14	$y = 1.77\ln(x) + 0.82$	0.37	$y = 3.02\ln(x) + 10.80$
Pine	0.22	$y = 3.29\ln(x) - 1.42$	0.20	$y = 2.99\ln(x) + 14.45$
Oak	0.28	$y = 1.71\ln(x) + 0.40$	0.67	$y = 3.82\ln(x) + 14.27$

3.3 DIURNAL PATTERNS

On average, in 2018, over a 24-hour period, pines had the largest peak instantaneous sap flux ($20.9 \text{ g}_{\text{H}_2\text{O}} \text{ m}^{-2}_{\text{sapwood}} \text{ s}^{-1}$) followed by junipers ($11.8 \text{ g}_{\text{H}_2\text{O}} \text{ m}^{-2}_{\text{sapwood}} \text{ s}^{-1}$), and then by oaks ($10.5 \text{ g}_{\text{H}_2\text{O}} \text{ m}^{-2}_{\text{sapwood}} \text{ s}^{-1}$) (Figure 11A). Oaks and junipers exhibited a consistent temporary decrease in midmorning sap flux: between 9:30-10:30 for the junipers and 10:30-11:30 for oaks (Figure 11A). Pines exhibited a minor reduction in the slope of the line from 9:00-10:00 indicating a decrease in flow. At 18:30, all species increased flow until 19:30 when it began to decline as PAR approached zero (Figure 11A). Similarly, in 2019, pines maintained the same relative sap flux magnitude ($22.2 \text{ g}_{\text{H}_2\text{O}} \text{ m}^{-2}_{\text{sapwood}} \text{ s}^{-1}$), or maximum rate (Figure 11B). Conversely, to 2018, oaks had greater peak diurnal flux ($12.9 \text{ g}_{\text{H}_2\text{O}} \text{ m}^{-2}_{\text{sapwood}} \text{ s}^{-1}$) than junipers ($11.6 \text{ g}_{\text{H}_2\text{O}} \text{ m}^{-2}_{\text{sapwood}} \text{ s}^{-1}$) until ~13:30, at which point the oaks decrease more rapidly (Figure 11B). At 18:30, both junipers and oaks saw an increase in sap flux (Figure 11). The oak flux began to decrease at hour 19:30, and juniper flux began to decrease at 20:00 (Figure 11). Pines likewise experienced a marginal increase in flux at 18:30 but resume their decline at 19:30 (Figure 11B).

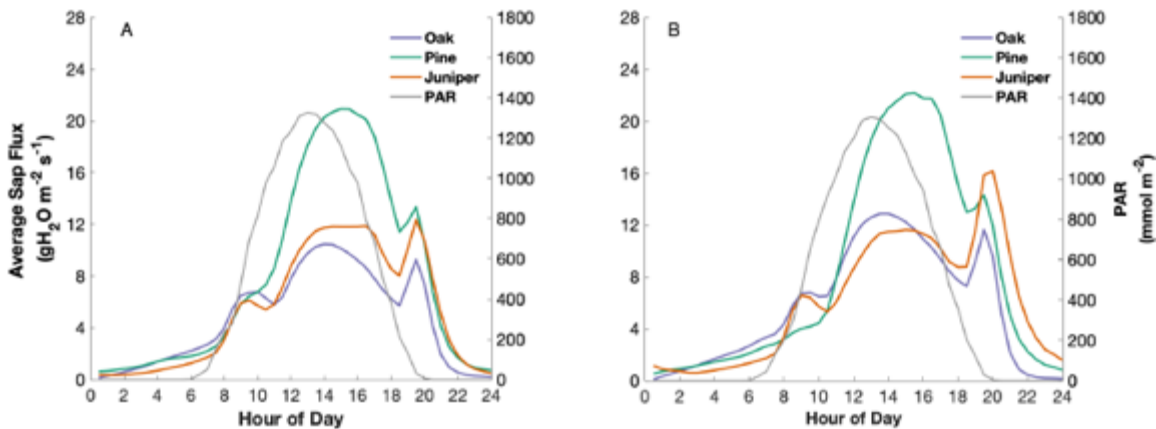


Figure 11: Average instantaneous sap flux over diurnal period by species for 2018 (A) and 2019 (B) from DOY 120-300.

3.3.1 Diurnal Patterns among Tree Size Classifications

3.3.1a Juniper

When further distinguished by tree size, the results show medium sized ($13 \text{ cm} \leq \text{DBH} \leq 24 \text{ cm}$) juniper trees had, on average, higher sap flux than large junipers ($\text{DBH} > 24 \text{ cm}$) for both 2018 and 2019 (Figure 12). Both size categories demonstrate similar diurnal patterns in sap flux characterized by a small decline around mid-morning, $\sim 10:00$ for large juniper, and $\sim 10:30$ for medium (Figure 12). Likewise, both size categories demonstrate an increase in sap flux occurring in the evening around $18:30$ (Figure 12). This increase was substantially larger in 2019 than in 2018. In 2018, large junipers had a slightly higher midday peak sap flux ($10.8 \text{ g}_{\text{H}_2\text{O}}\text{m}^{-2}_{\text{sapwood}}\text{s}^{-1}$) (Figure 12A) than 2019 ($8.6 \text{ g}_{\text{H}_2\text{O}}\text{m}^{-2}_{\text{sapwood}}\text{s}^{-1}$) (Figure 12B) with the midday peak shifted from $13:30$ to $16:30$. The magnitude of the midday peak for medium junipers was similar between 2018 ($16.0 \text{ g}_{\text{H}_2\text{O}}\text{m}^{-2}_{\text{sapwood}}\text{s}^{-1}$) and 2019 ($15.5 \text{ g}_{\text{H}_2\text{O}}\text{m}^{-2}_{\text{sapwood}}\text{s}^{-1}$).

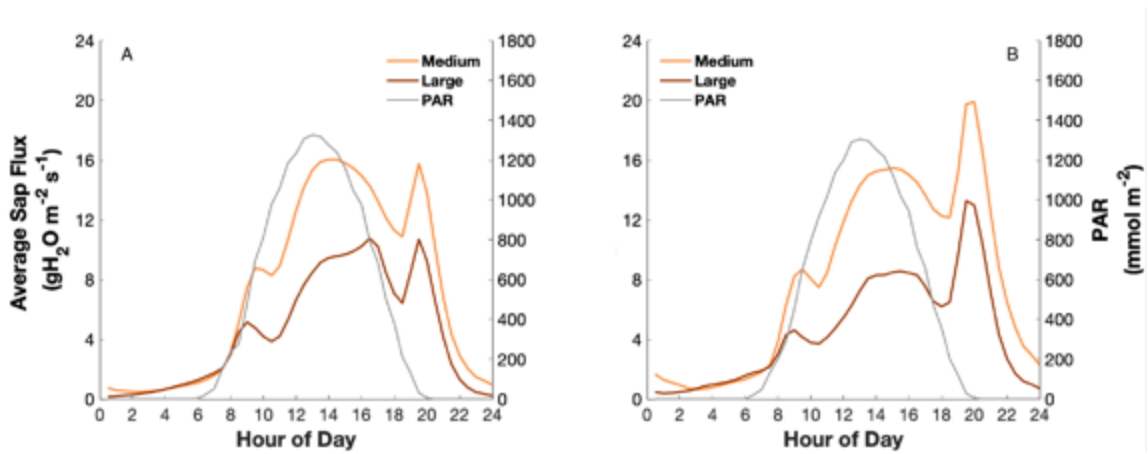


Figure 12: Average instantaneous sap flux over diurnal period for juniper from 2018 (A) and 2019 (B) DOY 120-300 by medium ($13 \text{ cm} \leq \text{DBH} \leq 24 \text{ cm}$) and large ($\text{DBH} > 24 \text{ cm}$) size classifications.

3.3.1b Pine

Large pines in 2018 and 2019 had higher midday fluxes (32.0 and $27.5 \text{ gH}_2\text{O m}^{-2} \text{ sapwood s}^{-1}$) with later peaks ($15:30$) than medium-sized pines (7.9 and $2.8 \text{ gH}_2\text{O m}^{-2} \text{ sapwood s}^{-1}$) ($12:30$) (Figure 13). During 2019, medium pines had lower fluxes, with a steady decline in flux after the midday peak (Figure 13B); whereas in 2018, fluxes from medium pines declined more slowly (Figure 13A). All pines, regardless of size, demonstrated a characteristic peak at $18:30$ in both years.

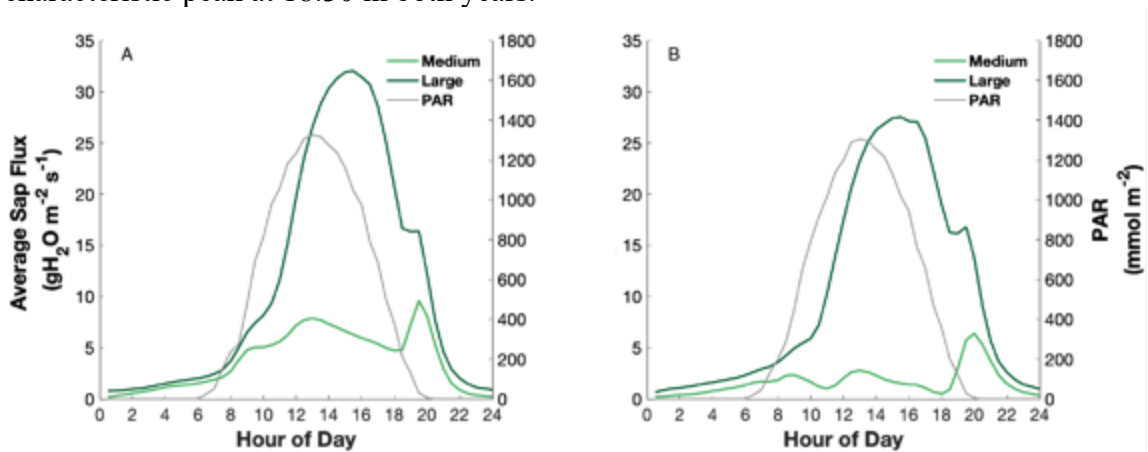


Figure 13: Average instantaneous sap flux over diurnal period for pines from 2018 (A) and 2019 (B) DOY 120-300 by medium ($13 \text{ cm} \leq \text{DBH} \leq 24 \text{ cm}$) and large ($\text{DBH} > 24 \text{ cm}$) size classifications.

3.3.1c Oak

Medium oaks, on average, had three diurnal peaks in flux occurring at 10:00, 13:30, and 19:30 (Figure 14). The large oaks in 2018 gradually increased flux until 09:00 when it increased more quickly until the midday peak at 14:00 (Figure 14A). In 2019, large oaks showed a rapid increase of sap flux occurring at 8:00 when PAR was increasing rapidly (Figure 14B). The large oaks in 2019 had a greater midday peak ($126.4 \text{ g}_{\text{H}_2\text{O}}\text{m}^{-2}\text{sapwoodS}^{-1}$) than large oaks in 2018 ($10.2 \text{ g}_{\text{H}_2\text{O}}\text{m}^{-2}\text{sapwoodS}^{-1}$), and medium oaks in 2018 and 2019 (10.8 and $9.4 \text{ g}_{\text{H}_2\text{O}}\text{m}^{-2}\text{sapwoodS}^{-1}$). Both size categories of oaks in 2019 exhibited a midday drop in flux at 10:30, and a peak at 19:00 with the large oaks having a greater increase in magnitude (Figure 14B).

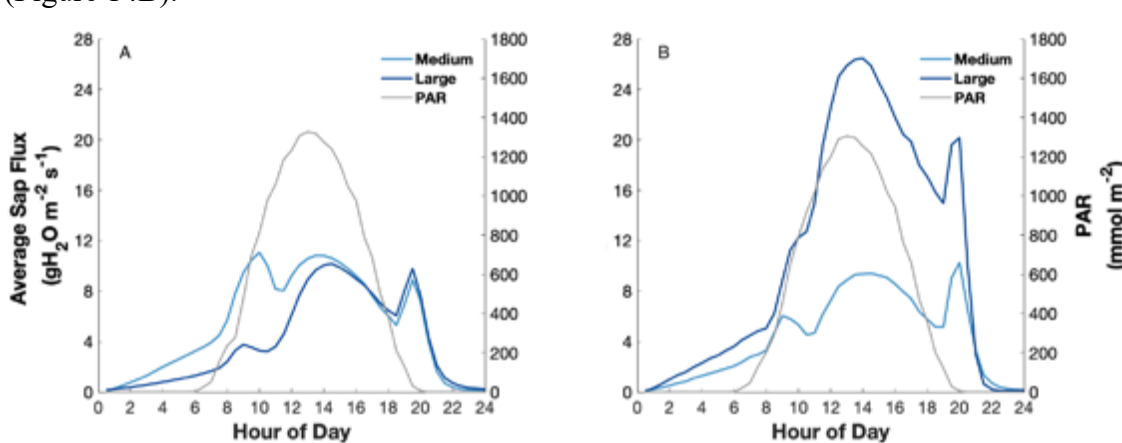


Figure 14: Average instantaneous sap flux over diurnal period for oaks from 2018 (A) and 2019 (B) DOY 120-300 by medium ($13 \text{ cm} \leq \text{DBH} \leq 24 \text{ cm}$) and large ($\text{DBH} > 24 \text{ cm}$) size classifications.

3.3.2 Wet and Dry Conditions

To identify possible species-specific relationships between transpiration and soil water content, we compared a wet and a dry seven-day period from 2018. The average soil water content (SWC) during the wet period ranged from 0.309 to $0.511 (\text{m}^3\text{H}_2\text{O m}^{-3} \text{ soil})$ (Table 8), more than double the mean SWC for the year. The average SWC during the dry period ranged from 0.120 to $0.147 (\text{m}^3\text{H}_2\text{O m}^{-3} \text{ soil})$, roughly half of the mean annual SWC

for 2018. On average, air temperature during dry soil conditions was 2.1 °C warmer than during the wet conditions. VPD during dry soil conditions was 25.7% greater than during wet conditions (Table 8).

Table 8: Mean hydro-meteorological values for seven day wet (SWC > 0.3 m³H₂O m⁻³ soil) and dry periods (SWC < 0.2 m³H₂O m⁻³ soil). The standard deviation of the mean values is given in parentheses. Percent change was calculated based on the difference between wet conditions and dry conditions.

Hydro-meteorological Parameters			
	Wet (DOY 141-147)	Dry (DOY 164-170)	Percent Change (%)
Temperature (°C)	25.6 (±5.0)	27.7 (±4.0)	8.3
Total Precipitation (mm)	0.00	0.00	-
Vapor Pressure Deficit (kPa)	1.37 (±1.12)	1.72 (±1.05)	25.7
Soil Water Content (m³ H₂O m⁻³ soil)	0.398 (±0.057)	0.133 (±0.007)	-66.7
Relative Humidity (%)	85.6 (±20.0)	58.7 (±18.0)	-31.4

3.3.2a Juniper

During dry conditions, junipers decrease midmorning sap flux at ~11:00 (Figure 15A). Medium junipers' curve, during wet conditions, has a minor leveling of the slope and the large junipers experienced a brief decrease in flux (Figure 15B). Medium-sized junipers experienced a larger reduction in transpiration during dry conditions (49.2%) than their larger counterparts (4.0%) (Figure 15). During wet conditions, the midday peak in

flux for medium and large junipers (28.0 and $20.6 \text{ g}_{\text{H}_2\text{O}}\text{m}^{-2}\text{sapwood}\text{s}^{-1}$) (Figure 15B) occurs between 14:00-15:00 but is shifted slightly earlier in the day during dry conditions to 11:30-12:00 (16.7 and $13.0 \text{ g}_{\text{H}_2\text{O}}\text{m}^{-2}\text{sapwood}\text{s}^{-1}$) (Figure 15A). All junipers in both wet and dry conditions show a similar evening spike in sap flux at 18:30 (Figure 15).

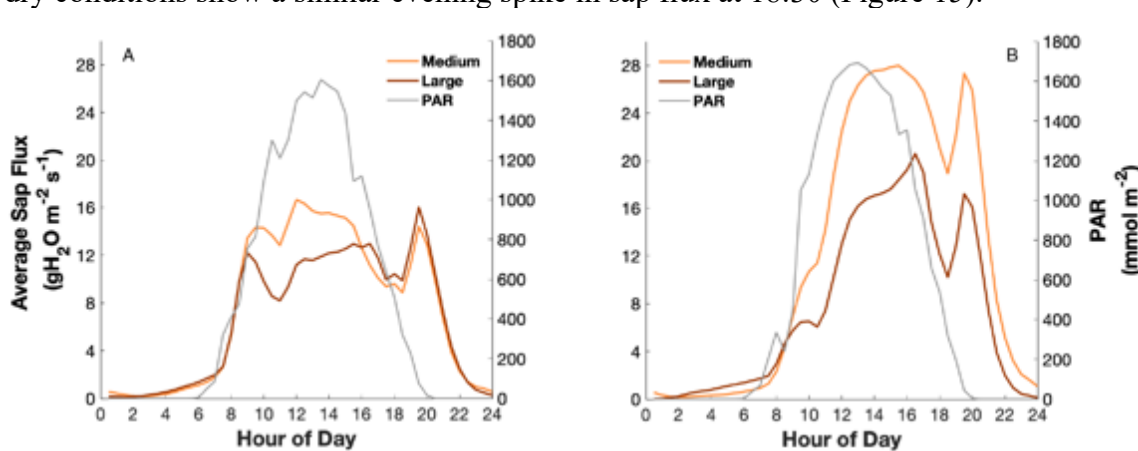


Figure 15: Average instantaneous sap flux over diurnal period for junipers during 7-day period for dry conditions when $\text{SWC} < 0.2 \text{ m}^3\text{H}_2\text{O m}^{-3}$ (A) and wet conditions when $\text{SWC} > 0.3 \text{ m}^3\text{H}_2\text{O m}^{-3}$ (B) by medium ($13 \text{ cm} \leq \text{DBH} \leq 24 \text{ cm}$) and large ($\text{DBH} > 24 \text{ cm}$) size classifications.

3.3.2b Pine

Both medium and large pines had higher midday values during wet conditions (24.5 and $59.1 \text{ g}_{\text{H}_2\text{O}}\text{m}^{-2}\text{sapwood}\text{s}^{-1}$) (Figure 16B) than dry conditions. The midday peaks for both sizes dropped during dry conditions (4.9 and $29.0 \text{ g}_{\text{H}_2\text{O}}\text{m}^{-2}\text{sapwood}\text{s}^{-1}$) and shifted to earlier in the day (Figure 16A). During dry conditions, pines exhibited a large decrease in peak daily sap flux ($\sim 50\%$ for large and 75% for medium) at midday (Figure 16A). The average daily transpiration decreased by 68.3% for medium pines and 42.1% for large pines between wet and dry conditions. Medium and large pines showed a spike in flux at 18:30 during both wet and dry conditions (Figure 16).

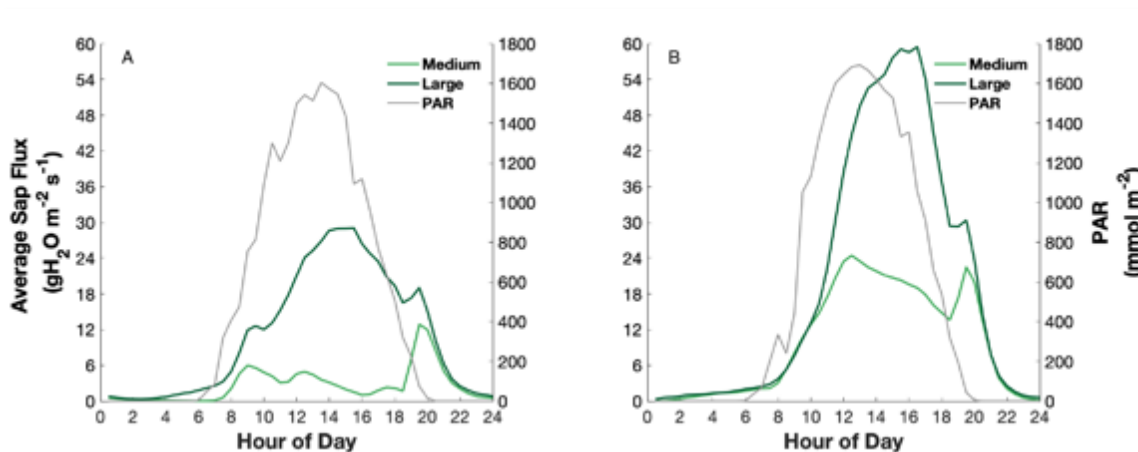


Figure 16: Average instantaneous sap flux over diurnal period for pines during 7-day period for dry conditions when SWC < 0.2 m³H₂O m⁻³(A) and wet conditions when SWC > 0.3 m³H₂O m⁻³ (B) by medium (13 cm ≤ DBH ≤ 24 cm) and large (DBH > 24 cm) size classifications.

3.3.2c Oak

During dry conditions, medium-sized oaks shifted sap flux to the morning hours with a strong peak at 9:00, followed by a decline for the majority of the day, until an evening spike at 20:00 (Figure 17A). In dry conditions, large oaks demonstrated a marginal decline in flux at midmorning, rebounded during the peak of the day (12:00-15:00), declined temporarily and peaked again in the evening at the same time as the medium-sized cohort (Figure 17A). Similarly to dry conditions, during wet conditions, medium-sized oaks showed a strong skew towards morning transpiration, and transpired more than their larger counterparts during this period (Figure 17B). Sap flux from large oaks was more temporally aligned with PAR than the medium oaks during wet conditions. However, the evening (20:00) spike in flux was conserved across all tree sizes (Figure 17). Midday peaks during dry conditions were similar for medium and large oaks (10.3 and 11.4 g_{sapwood}m⁻²s⁻¹) (Figure 17A). Peak sap flux was slightly higher during wet conditions for both medium and large oaks (11.9 and 13.2 g_{sapwood}m⁻²s⁻¹) (Figure 17B). Medium oaks

experienced a 7.6% increase in daily transpiration between dry and wet conditions while large oaks had a smaller decrease (4%).

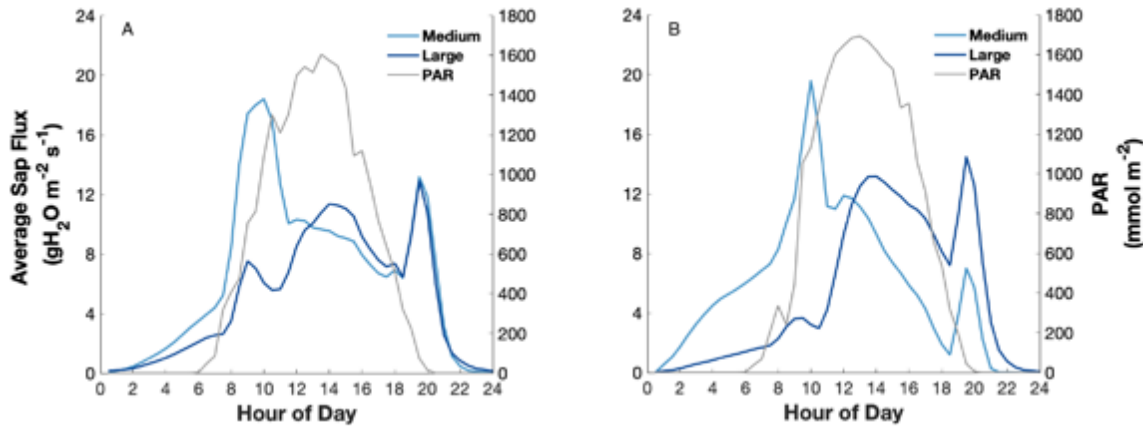


Figure 17: Average instantaneous sap flux over diurnal period for oaks during 7-day period for dry conditions when $SWC < 0.2 \text{ m}^3\text{H}_2\text{O m}^{-3}$ (A) and wet conditions when $SWC > 0.3 \text{ m}^3\text{H}_2\text{O m}^{-3}$ (B) by medium ($13 \text{ cm} \leq DBH \leq 24 \text{ cm}$) and large ($DBH > 24 \text{ cm}$) size classifications.

3.3.3 Transpiration responses to partial clearing of *J. ashei*

In 2018, before the partial clearing of *J. ashei* from the site, pines transpired more than the other species (12.1 kg day^{-1}) followed by junipers (10.9 kg day^{-1}) and finally oak (6.4 kg day^{-1}) (Table 9). After partial clearing took place in 2019 (DOY 84-106), pines continued to transpire more than any other species, and more than their average in 2018 (14.7 kg day^{-1}), followed by juniper (12.5 kg day^{-1}), and oak (10.0 kg day^{-1}) (Table 9). On average, all species had higher transpiration rates in 2019 than in 2018 (Table 9).

Medium and large junipers experienced the least change in sap flux volumes between pre- and post- clearing with an 11.5% and 16.3% increase respectively. Decreases in transpiration were seen for medium oaks (-14.4%) and medium pines (-48.9%). After clearing, large oaks exhibited the largest increase in transpiration, at 201%, of any species-size category. Overall, all species exhibited an increase transpiration between 2018 and

2019, with oaks registering the largest increase (55.7%), followed by pines (21.5%), and junipers (14.5%) (Table 9). For the entire project period (DOY 120-300 of 2018 through DOY 120-300 of 2019) transpiration for pines averaged 12.5 kg day⁻¹, juniper 11.4 kg day⁻¹, and oaks 7.6 kg day⁻¹(Table 9).

Table 9: Average transpiration rates pre- (2018), postclearing (2019), and the average of both years by species and medium (13 cm ≤ DBH ≤ 24 cm) and large (DBH > 24 cm) size classifications.

Amount of Transpiration, DOY 120-300					
		2018	2019	2018 and 2019 Average	Percent Change Between 2018 and 2019 (%)
Juniper (kg day⁻¹)	Medium	10.5	11.7	10.9	11.5
	Large	11.2	13.1	11.8	16.3
	Average	11	12.5	11.4	14.5
Pine (kg day⁻¹)	Medium	4.7	2.4	4.1	-48.9
	Large	23.2	27	25	16.4
	Average	12.1	14.7	12.5	21.5
Oak (kg day⁻¹)	Medium	4.3	3.7	3.9	-14.4
	Large	9.6	28.9	13.1	201
	Average	6.4	10	7.6	55.7

3.3.4 Elevation change and sap flux

3.3.4a Juniper

We compared sap flux in trees of similar species and size (within 1.50 cm DBH) spanning the elevation gradient at the site before and after partial clearing. The elevation gradient between Juniper 7 and Juniper 10 is ~5.8 meters. Prior to clearing Juniper 7 (low elevation) (10.9 kg day^{-1}) transpired less on average than Juniper 10 (high elevation) (13.0 kg day^{-1}) (Figure 18A). After clearing, the two trees sap flux was roughly equal (Figure 18B). Transpiration increased for Juniper 7 (Low) by 48.7% and Juniper 10 (High) by 17.3% after the clearing.

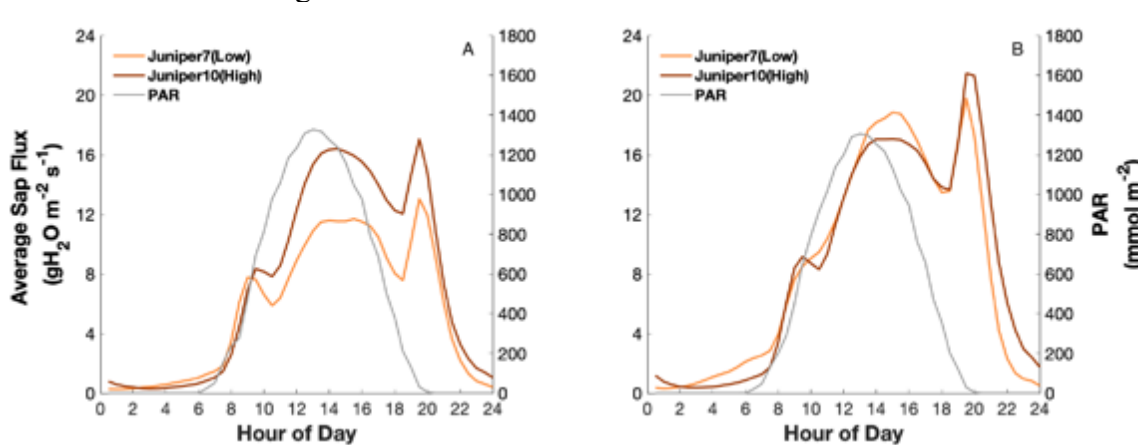


Figure 18: Elevation influences on diurnal sap flux patterns for an up slope tree (Juniper 10) elevation 637.3 m, and a down slope tree (Juniper 7) elevation 631.5 m during 2018 (A) and 2019 (B).

3.3.4b Pine

Both high and low elevation pines decreased average daily sap flux after the juniper clearing (Figure 19). The elevation gradient between Pine 1 and Pine 6 is 1.6 meters. The diurnal pattern changed dramatically after the clearing for both pines (Figure 19B). Pine 1 (low elevation) sap flux decreased at ~11:00, then peaking at 12:00 before decreasing from 13:00-18:00 with a sharp evening peak that occurred at 18:00 (Figure 19B). Pine 6

(high elevation) sap flux decreased at ~09:30, peaked at ~13:00, and decreased again from 14:00-18:00 with a similar spike to Pine 1 (Figure 19B). Pine 6 (high) had a decrease in transpiration by 45.5% and pine 1(low) decreased by 61.0% post clearing.

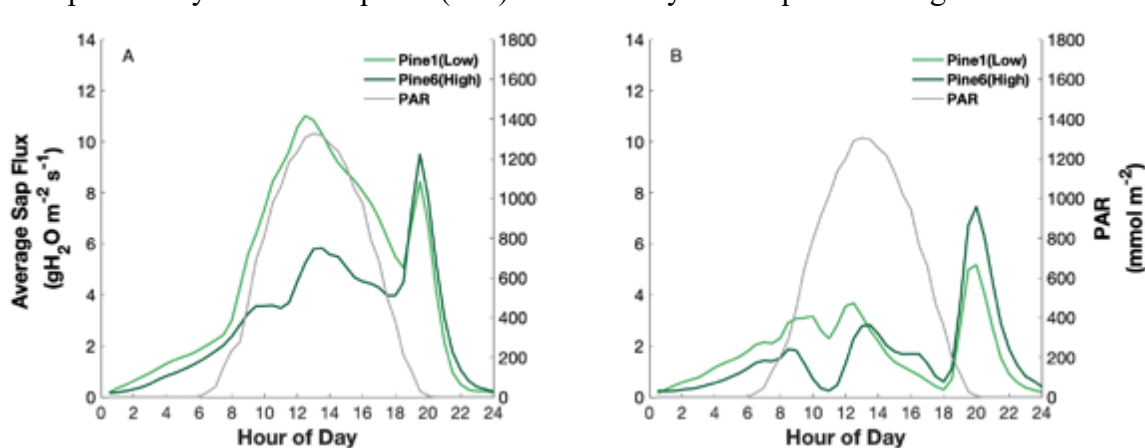


Figure 19: Elevation influences on diurnal sap flux patterns for an up slope tree (Pine 6) elevation (638.5m), and a down slope tree (Pine 1) elevation (636.9 m) during 2018 (A) and 2019 (B) with a one hour moving average applied.

3.3.4c Oak

In 2018, the midday peak of sap flux for Oak 3 (high elevation) occurred at ~13:30 ($6.4 \text{ gH}_2\text{O m}^{-2} \text{ sapwood s}^{-1}$) and shifted in 2019 to ~14:30 ($13.4 \text{ gH}_2\text{O m}^{-2} \text{ sapwood s}^{-1}$) (Figure 20). In contrast the midday peak sap flux for Oak 1(low elevation) shifted from ~13:30 in 2018 ($15.2 \text{ gH}_2\text{O m}^{-2} \text{ sapwood s}^{-1}$) to ~13:00 in 2019 ($9.8 \text{ gH}_2\text{O m}^{-2} \text{ sapwood s}^{-1}$) (Figure 20). Midday sap flux values for Oak 1(low) were higher in 2019 than 2018, whereas midday sap flux for Oak 3 (high) was higher in 2018 than 2019 (Figure 20). Oak 1 (low) increased in transpiration by 26.0% while Oak 3 (high) decreased by 18.2% post clearing. The elevation gradient between Oak 1 and Oak 3 is 1 meter.

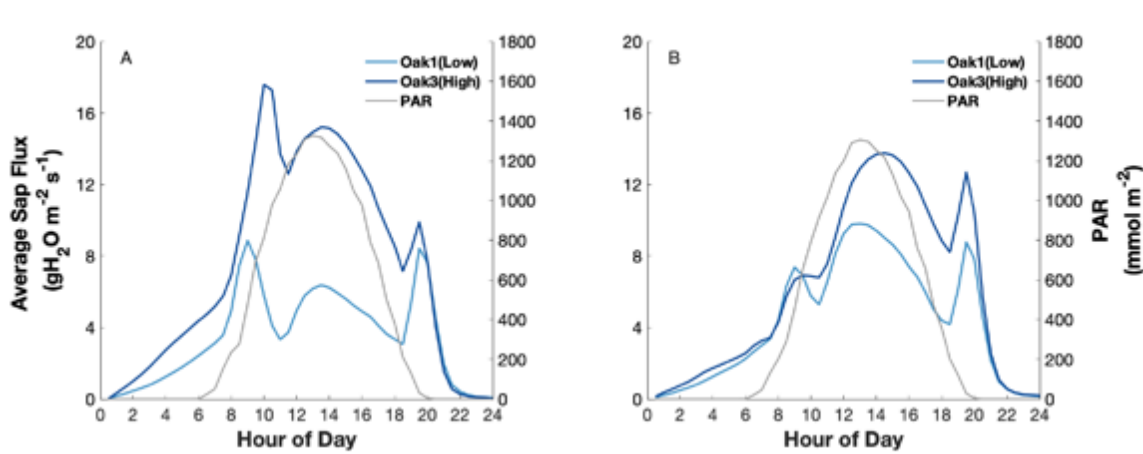


Figure 20: Elevation influences on diurnal sap flux patterns for an up slope tree (Oak 3) elevation 638.3 m, and a down slope tree (Oak 1) elevation 637.3 m during 2018 (A) and 2019 (B).

3.4 LEAF WATER POTENTIAL MEASUREMENTS

3.4.1 Leaf Water Potential vs. Vapor Pressure Deficient

Leaf water potential is used as a metric for the hydration status of individual leaves. More negative values indicate increasing water stress, while values close to zero indicate well hydrated conditions. Leaf water potential (ψ_L) responds to atmospheric demand for moisture (VPD) as well as water availability at the roots ultimately governed by SWC. We measured two juniper trees one at the bottom of the hillslope “juniper low” and the other “juniper” is at an elevation similar to that of the oak and pine. Pre-dawn pine and oak ψ_L remained near -0.6 MPa while junipers, both upslope and downslope, were near -0.7 MPa (Table 10). Measurements of ψ_L taken before dawn on pine ($R^2 = 0.36$ and $P = 3.78e-02$) and oak ($R^2 = 0.78$ and $P = 1.54e-03$) became less negative as VPD increased (Figure 21). At midday (12:00), ψ_L becomes increasingly negative with increasing atmospheric demand, as expected. This relationship is significant for oak ($R^2 = 0.99$ and $P = 9.40e-06$) and juniper ($R^2 = 0.82$ and $P = 4.89e-05$) (Figure 21). Oaks experienced the most negative noontime ψ_L values near -3.5 MPa, pine averaged to approximately -1.5 MPa and juniper

was -2.0 MPa while juniper low was slightly less at -1.9 MPa (Table 10). Afternoon ψ_L (16:00) for pine ($R^2 = 0.39$ and $P = 2.88e-02$) and oak ($R^2 = 0.73$ and $P = 3.13e-02$) had a positive relationship with VPD (Figure 21 and Table 11). Afternoon pine ψ_L remained around -1.5 MPa while oak and the low elevation juniper became less negative with averages near -1.5 MPa, and up-slope juniper remained near -2.0 MPa (Figure 21 and Table 10). All trees had less negative ψ_L during the evening (18:00) with oaks at a similar pressure to their dawn values of -0.5 MPa (Figure 21 and Table 10). Throughout the day, the upslope juniper had consistently more negative ψ_L than the downslope juniper (Figure 21 and Table 10).

Table 10: Leaf water measurements taken in triplicate and averaged with the standard deviation in the parentheses. Measurements that are italicized were taken during overcast conditions, and evening measurements were conducted after the sun had set but prior to full dark conditions.

Leaf Water Potential Measurements (MPa)					
		Pine	Oak	Juniper	Juniper Low
2/2/20	Dawn	-0.67 (\pm 0.10)	-0.73 (\pm 0.07)	-0.63 (\pm 0.04)	-0.73 (\pm 0.04)
2/3/20	Dawn	-0.64 (\pm 0.01)	-0.39 (\pm 0.04)	-0.77(\pm 0.02)	-0.74 (\pm 0.03)
3/7/20	Dawn	-0.58 (\pm 0.02)	-0.37 (\pm 0.05)	-0.58 (\pm 0.04)	-0.65 (\pm 0.02)
3/8/20	Dawn	-0.68 (\pm 0.03)	-	-0.67 (\pm 0.06)	-0.73 (\pm 0.04)
2/1/20	Noon	-2.31 (\pm 0.19)	-3.45 (\pm 0.17)	-1.99 (\pm 0.11)	-1.73 (\pm 0.12)
2/2/20	Noon	-1.43 (\pm 0.17)	=	-2.10 (\pm 0.09)	-1.73 (\pm 0.10)
3/7/20	Noon	-1.49 (\pm 0.10)	=	-1.72 (\pm 0.04)	-1.57(\pm 0.03)
3/8/20	Noon	-0.85 (\pm 0.08)	-0.65 (\pm 0.04)	-0.87 (\pm 0.08)	-
2/1/20	Afternoon	-0.84 (\pm 0.10)	-1.44 (\pm 0.16)	-2.10 (\pm 0.11)	-1.33 (\pm 0.10)
2/2/20	Afternoon	-1.27 (\pm 0.04)	-1.01 (\pm 0.05)	-1.80 (\pm 0.09)	-1.58 (\pm 0.08)
3/6/20	Afternoon	-1.60 (\pm 0.05)	-1.30(\pm 0.05)	-1.95 (\pm 0.05)	-1.66 (\pm 0.09)
3/7/20	Afternoon	-1.90 (\pm 0.10)	-1.84 (\pm 0.14)	-1.83 (\pm 0.15)	-1.37 (\pm 0.01)
2/1/20	Evening	-0.96 (\pm 0.14)	-0.57 (\pm 0.08)	-1.08 (\pm 0.04)	-0.89 (\pm 0.11)
2/2/20	Evening	-1.18 (\pm 0.05)	-0.75 (\pm 0.02)	-1.21(\pm 0.02)	-0.97 (\pm 0.04)
3/6/20	Evening	-1.06 (\pm 0.10)	-0.67 (\pm 0.08)	-1.23 (\pm 0.08)	-0.60 (\pm 0.03)
3/7/20	Evening	-1.43 (\pm 0.12)	-0.62 (\pm 0.05)	-1.55 (\pm 0.08)	-1.20 (\pm 0.00)

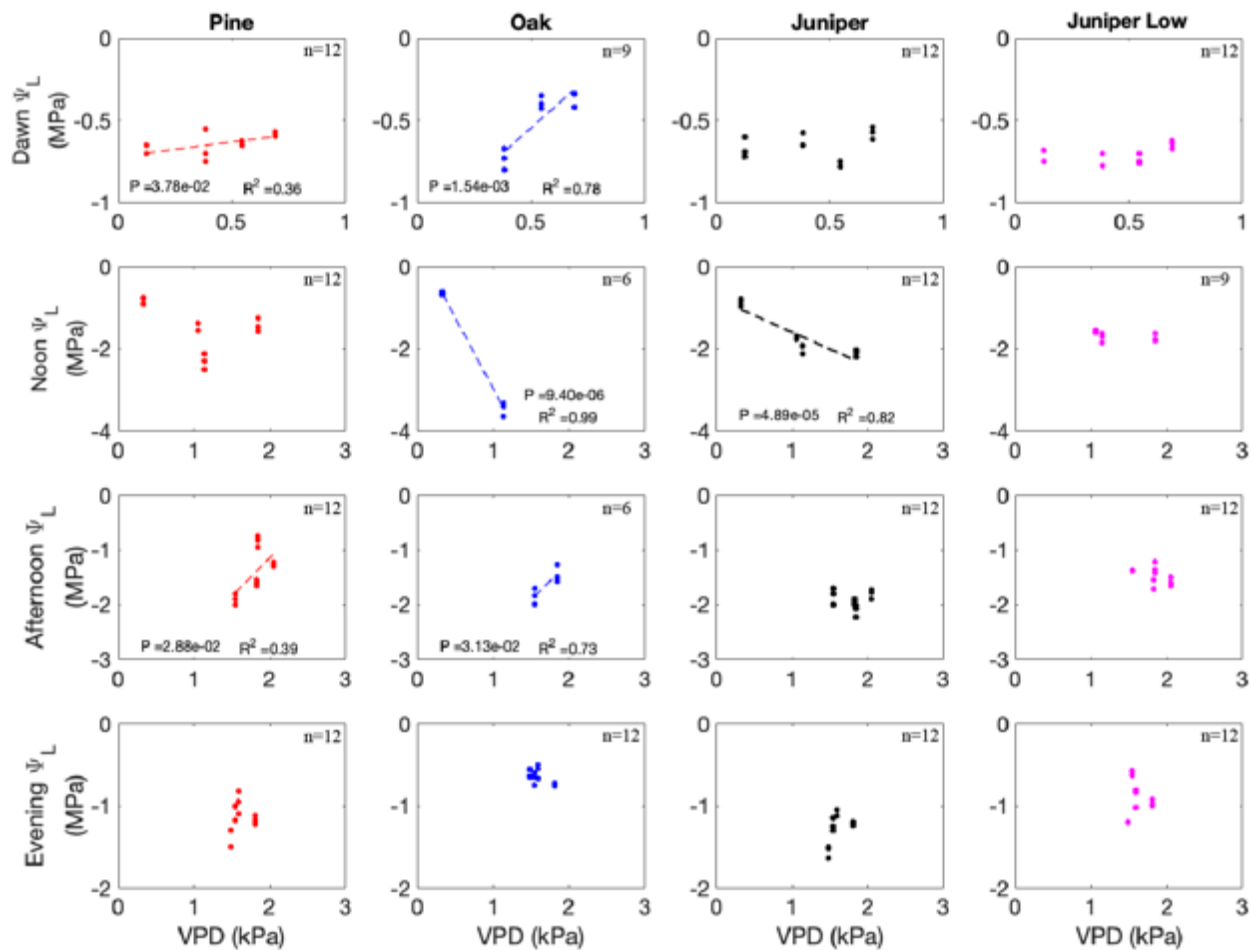


Figure 21: Leaf water potential (ψ_L) compared with atmospheric demand for water vapor (VPD). The pine, oak, and juniper are located at similar elevations in the upper portion of the slope, and “Juniper Low” was located at the bottom of the hillslope. The number (n) of measurements for each sampling period and tree is given in the top right of each plot. Significant P and R^2 values were added to each plot.

Table 11: Slope values for leaf water potential plotted against VPD for each sampling period. Relationships that were not significant are shown as (-).

Equations for LWP vs VPD lines of best fit				
	Pine	Oak	Juniper	Juniper Low
Dawn	$y = 0.17x - 0.72$	$y = 1.21 - 1.15$	-	-
Noon	-	$y = -3.45x + 0.48$	$y = -0.82x - 0.77$	-
Afternoon	$y = 1.40x - 3.94$	$y = 1.34x - 3.91$	-	-
Evening	-	-	-	-

3.4.2 Leaf Water Potential and Soil Water Content

At dawn, ψ_L was only significantly related to SWC for oaks ($R^2 = 0.78$ and $P = 1.67e-03$) (Figure 22). Surprisingly, oak ψ_L decreased (becomes more negative, i.e. more stressed) as soil water content increased (Figure 22). During noon, pine ($R^2 = 0.91$ and $P = 1.70e-06$), oak ($R^2 = 0.99$ and $P = 9.40e-06$), and juniper ($R^2 = 0.80$ and $P = 9.22e-05$) all showed negative relationships between ψ_L and SWC (Figure 22 and Table 12). Afternoon ψ_L in pine ($R^2 = 0.91$ and $P = 1.70e-06$) and oak ($R^2 = 0.73$ and $P = 3.13e-02$) demonstrated strong positive relationships, indicating that leaves became more stressed with drier soil, as typically expected (Figure 22 and Table 12). Pine ($R^2 = 0.68$ and $P = 8.94e-04$) and juniper ($R^2 = 0.90$ and $P = 2.22e-6$) demonstrated significant positive relationships between ψ_L and SWC in the evening (Figure 22 and Table 12)..

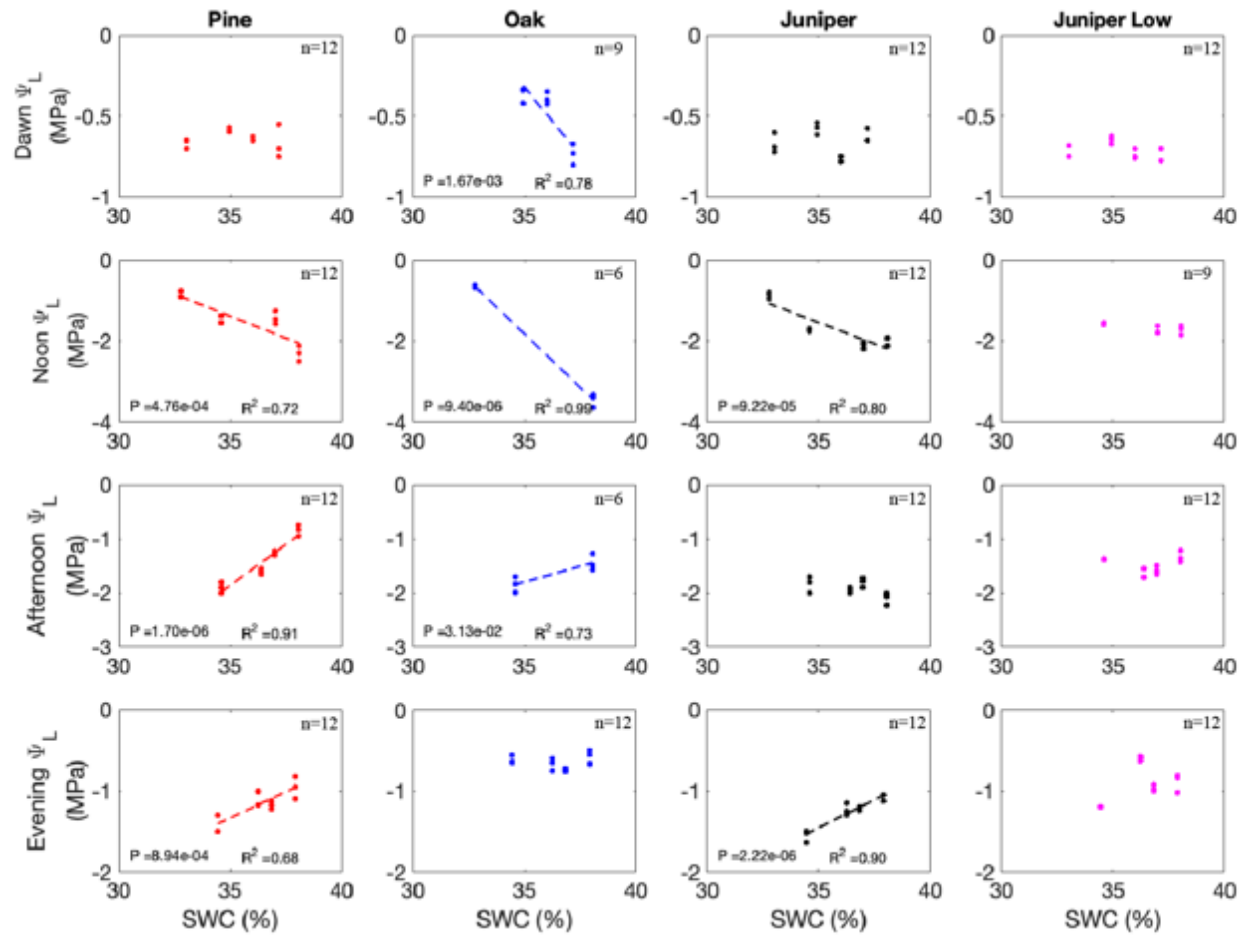


Figure 22: ψ_L as compared to SWC. The pine, oak, and juniper are located at similar elevations in the upper portion of the slope, and “Juniper Low” was located at the bottom of the hillslope. The number (n) of measurements for each sampling period and tree is given in the top right of each plot. Significant P and R^2 values were added to each plot.

Table 12: Slope values for leaf water potential plotted against SWC for each sampling period. Relationships that were not significant are shown as (-).

Equations for LWP vs SWC lines of best fit				
	Pine	Oak	Juniper	Juniper Low
Dawn	-	$y = -0.17x + 5.54$	-	-
Noon	$y = -0.22x + 6.25$	$y = -0.53x + 16.70$	$y = -0.21x + 5.83$	-
Afternoon	$y = 0.30x - 12.50$	$y = 0.12x - 5.83$	-	-
Evening	$y = 0.13x - 5.88$	-	$y = 0.14x - 6.23$	-

3.5 VISUAL INCREASES IN SPRING WATER

A small spring exists at the bottom of the hillslope that was barely outputting water, just enough to form a small pool. Noticable visual observations of increased flow occurred after the clearing, and the extent of the pool expanded ~75 meters down the otherwise dry stream channel. Water levels did not change noticeably during the 2019 drought. However, the flow from the spring remained so low that measurements were not possible.

Chapter 4: Discussion

4.1 PRE- POST- CLEARING TRANSPIRATION CHANGES

Our results provide new insights surrounding the debate on the benefits of ashe juniper removal in the Edwards Plateau by examining sap flux and transpiration changes pre- and post- clearing. Transpiration increased after the clearing for the entire 2019 growing season for junipers, oaks, and pines (Figure 6 and Figure 7). However, this increase in transpiration was not evident within the 13-day comparison window selected to eliminate the influence of meteorological variability. During this period, transpiration from junipers and pines decreased while transpiration from oaks increased (Figure 8, Figure 9, and Table 6). While we endeavored to pick a window with similar meteorological conditions pre- and post- clearing, conditions in 2019 were consistently drier than in 2018 and some discrepancies were unavoidable. The 13-day period in 2019 had an average SWC that was nearly 18% lower than the 2018 comparison window

Table 5). In 2019, all species showed stronger relationships between sap flux and soil moisture than in 2018 (Figure 10B). While both sites had similar precipitation amounts prior to the comparison period, the precipitation event in 2018 occurred as two separate events leading to a prolonged increase in soil water availability and therefore transpiration (Figure 6 and Figure 7). Oaks increased transpiration during both the full growing season and 13-day comparison window suggesting that this species benefitted from the removal of upslope juniper (Table 6 and Table 9). One potential explanation for the disproportionate impact to oak transpiration is the location of the clearing relative to the instrumented trees. The majority of juniper removal occurred at the highest elevations of the watershed and specifically along ridge tops (Figure 1). Our instrumented large oaks are clustered along

the banks of a dry, upslope creek bed. The biomass from the felled junipers was left on the slope to slow runoff and promote infiltration down the slope. It is likely that the site topography helped direct water to the topographic low of the dry, upslope creek bed and thereby to the large oaks.

The overall increase in transpiration during the growing season for all species supports our third hypothesis that water availability to other species would increase after juniper clearing. The observed increase in sap flux and therefore transpiration in large oaks (Figure 8, Figure 9, and Table 9) indicates a substantial increase in root-zone moisture availability. The site-wide increase in growing season transpiration during a significantly drier year likewise indicates a positive effect of juniper removal (Table 9). A study by Dammeyer et al. (2016) compared a plot cleared of 90% of the ashe juniper trees to an unaltered control. In the cleared plot, sap flux increased by 80% in oak trees with minimal changes in juniper flux, similar to our results of ~56% and ~15% increase of oak and juniper sap flux, respectively. Comparable patterns of sap flux magnitude throughout the year along with a reduction of sap flux when SWC was near or below 20% were observed in the Dammeyer et al. (2016) study.

Throughout the study period, pines transpired the most water per individual followed by junipers, and then oaks (Table 9). However, in 2019 large oaks (28.9 kgday^{-1}) transpired more than the large junipers (13.1 kgday^{-1}), an increase likely due to a positive effect of juniper clearing and strategic positioning, or potentially an ability to root deeper. *Junipererus spp.* show a large range of transpiration rates depending on tree size and root water availability, with values near zero to 132 kg day^{-1} (Dammeyer et al., 2016; Kukowski et al., 2013; Owens, 1996; Starks et al., 2014). *Pinus edublis* another semi-arid species of pinyon pine showed that it transpires more than the sympatric *Junipererus osteosperma* (West et al., 2008). This is consistent with our results indicating that pinyon pine has the

capability to use more water than ashe juniper. The latter half of 2019 was classified as a drought year, causing reductions in transpiration for many individuals. We postulate that the heterogeneity of transpiration responses (increase or decrease) during 2019 is the result of differential access to subsurface water resources and potentially karst features. For instance, if the large oaks were only rooted in shallow soil, then they too would likely have experienced a decrease in transpiration during the dry soil conditions. The idea that oaks are more deeply rooted is supported by similar results from Dammeyer et al. (2016), which also found that oaks in the clearing were able to transpire longer into a drought year due to an increase in karst storage (Jackson et al., 1999).

4.2 TRANSPIRATION RESPONSE TO ENVIRONMENTAL CONDITIONS

4.2.1 Diurnal Sap Flux Response to Environmental Conditions

Daily cycles of sap flux vary in response to alterations in environmental conditions. Stomates open and close depending on changes in SWC, humidity, VPD, or light due to cloud cover variation (Bonan, 2019). An initial increase in morning sap flux for all species corresponds with increasing in PAR (Figure 15, Figure 16, Figure 17). The observed morning sap flux decreased at ~9:30 as a possible response of partial stomata closure in an effort to regulate and conserve the amount of water being transpired as sunlight and temperature increase during dry conditions (Figure 15A, Figure 16A, Figure 17A). The evening spike of sap flux that happened at ~19:00 for all species (Figure 14, Figure 15, and Figure 16) although to a lesser extent in large pines may not be transpiration but it could have been refilling of stem water to replenish trunk storage and prevent cavitation (Nadezhdina, 1999). Sap flux decreased at ~20:00 until it reached zero at ~24:00 (Figure 15, Figure 16, Figure 17). The decrease in flow during this time may be the result of: completion of stem water refill, the occurrence of nocturnal transpiration, or a combination

of the two (Fisher et al., 2007). Smaller dips and spikes in sap flux are also possible responses to changes stomatal opening reactions to changes in meteorological conditions. Potential explanation for the almost constant decrease in sap flux for the medium pines in the 7-day comparison is midday stomatal closure from low SWC and a higher VPD than wet conditions in an effort to prevent cavitation (Figure 16A and Table 8).

4.2.2 Vegetation Response to Drought

The strong relationships between transpiration and soil water content (Figure 10) indicate that all species at this site are highly dependent on shallow soil moisture. The shallow soil layer with a high ratio of rock fragments to soil medium results in the ability to store less water (Fies et al., 2002). Transpiration declined for all species-size cohorts except in large pines and large oaks indicating they may either exist in a location that permitted them to root deeply or have access to water-filled karst features (Bendevis et al., 2009; Estrada-Medina et al., 2013). The 2019 drought resulted in SWC that was consistently below 20% after DOY 190 and a notable decline in sap flux for junipers, some oaks, and some pines throughout the rest of the year, with the exception of short-lived responses to minor precipitation events (Figure 2). Kukowski et al. (2013) and Dammeyer et al. (2016) show similar responses of sap flow in oak to varying SWC and an overall higher juniper transpiration rate than oak. Junipers in the present study show a more rapid decline in sap flux in response to low SWC (Figure 9E) indicating a higher sensitivity to precipitation, while Kukowski et al. (2013) and Dammeyer et al. (2016) showed a gradual decrease of juniper sap flux over weeks. This decline in sap flux was commensurate with the region formally entering a drought that became more severe with time according to the PDSI. Oaks are known to have a higher tolerance to drought when able to root deeply and continue to transpire (Epron & Dreyer, 1993; Xu & Baldocchi, 2003). However, junipers

are known to continue transpiring at minimal levels during water stress in order to obtain small amounts of carbon for photosynthesis, while water limited oaks do not (Kukowski et al., 2013; Owens and Schreiber, 1992). Patterns of minimal transpiration have been observed for *J. osteosperma* and *Juniperus virginiana* both found in semiarid environments (Starks et al., 2014; West et al., 2007). Schwinning (2008) supports that with reduced SWC, juniper will continue to transpire albeit at very low values. The medium sized pines on site reduced transpiration by 68.3% during dry conditions (Figure 16). The reduction in transpiration is supported by a study by West et al. (2007) who found that during dry conditions transpiration of *Pinus edulis*, another semi-arid pinyon species, was greatly reduced to near zero to prevent xylem cavitation during drought. During periods of extreme soil water limitation (SWC < 20% for an extended period), a curious, but consistent, phenomenon was observed in diurnal sap flux trends. Sap flux increased from the time of day 00:00 through ~09:00, abruptly dropping to near zero until midday, then peaking around ~19:30 and decreased again until the following day. This pattern occurred for many of the medium trees of all species and the largest junipers when SWC was at 20% or below which is also approximately the permanent wilting point (19.7%) of the clay loam soil (Rawls et al., 1982). One hypothesis to explain the early morning and late evening/night increase is the refilling of xylem in an effort to prevent cavitation which can lead to permanent damage to the vascular tissue. If droughts become more severe and longer lasting, plants that are rooted deep enough to access water may survive while others would most likely be impacted by drought induced mortality via cavitation (Pangle et al., 2015).

We compared transpiration rates of pinyon pine, lacey oak, and ashe juniper and determined that, overall, pines transpired the most water per species followed by junipers and lastly oaks (Table 9). However, during the 2019 drought, oaks transpired more than the other species, followed by pines and finally junipers (Figure 7). This is in contrast to

patterns of transpiration observed during periods of 2018 and 2019 when moisture availability was not limiting.

4.3 TRANSPIRATION COMPARED TO ELEVATION, HILLSLOPE HYDROLOGY AND ROOTING DEPTH

4.3.1 Elevation Comparisons

Prior to the clearing, Juniper 7, located at the bottom of the hillslope, had lower sap flux values than Juniper 10, located at a higher elevation (Figure 18A). This trend changed post clearing when the lower elevation tree, Juniper 7, transpired, on average, a small amount more than the upslope Juniper 10 (Figure 18B). Pine 1 which is located at a lower elevation transpired more pre- and post-clearing than Pine 6 (Figure 19). Post clearing Pine 1 showed a reduction in transpiration but continued to transpire slightly more than Pine 1 (Figure 19B). The relationship between elevation and transpiration in oaks were opposite to that of pines. Oak 3, which is at a higher elevation, transpired more pre- and post-clearing than Oak 1, which is at a slightly lower elevation (Figure 20). Overall, there was no consistent trend that related elevation to sap flux between species. However, the natural variation in establishment at the site precludes a more robust analysis. Pines and oaks tend to be found only at higher elevations, while juniper is the only species to grow ubiquitously throughout the watershed.

4.3.2 Hillslope Hydrology

One potential explanation for the lack of a trend between transpiration rates and elevation is subsurface heterogeneity within the limestone bedrock. Water availability is heterogenous and has been reported to not correlate with elevation in karst due to subsurface profile differences (McCole & Stern, 2007; Tokumoto et al., 2014). This is reinforced by the understanding that rock water storage and porosity profiles can vary

beneath trees that exist next to each other at the same elevation (Tokumoto et al., 2014). A potential explanation for the observed differences in our site may be that the removal of the upslope junipers changed the hillslope hydrology of the basin, and the water table either rose or parts of the vadose zone were able to retain more moisture as storage in certain locations along preferred flow paths. The oaks located upslope and closest to the cleared area saw an increase in transpiration post-clearing. Therefore, oaks were able to maintain higher levels of sap flux during the driest soil conditions at the end of 2019 (Figure 7), suggesting that water was continuously available within their root zones. These oaks are also located near a dry creek bed that serves as a preferential flow path for runoff.

The second hypothesis of this study is that trees at higher elevations would transpire less because of greater depth to the water table. Our results are inconclusive in regard to this hypothesis. Elevation did not have a consistent effect on transpiration. However, microscale topography, such as the dry stream channel may play a significant role in determining subsurface hydrology.

4.3.3 Rooting Depth

The ability of large, upslope oaks to transpire more, post clearing, and in a drier year, indicated that juniper removal may have led to increased moisture availability within their root zone. Live oaks on the Edwards Plateau in Texas have been observed to root up to 22 meters deep and are able to uptake water at a depth of 18 meters (Jackson et al., 1999). In the same study, juniper roots were only found at depths shallower than 8 meters indicating that when possible oaks can extend their roots to greater depths for water. Junipers and oaks have also shown to develop dense root mats above the rock layer (~20 cm) with some of the roots weaving into small holes and cracks (Heilman et al., 2009; Schwinning, 2008), allowing for quick responses to small precipitation events like those

observed in this study (Figure 6 and Figure 7). Another study on the Edwards Plateau found similar patterns in root structure with a majority of ashe juniper roots occurring at or above 40 cm depth, with the occasional root extending deeper between fractures. In these studies, the majority of water uptake came within one meter of the surface (Elkington et al., 2014; Schwinning, 2008; Tokumoto et al., 2014). A study by Heilman et al. (2009) showed a strong correlation between evapotranspiration and near surface SWC indicating that the woodland relied more on water from recent rainfall than stored water in deeper layers or karst. These findings agree with the behaviors observed for medium pines and junipers which are characterized by strong increases in sap flux after rainfall, followed by a steady decrease in flux as SWC decreases (Figure 6 and Figure 7). Our results suggest deeper or more efficient rooting, by large oaks and large pines, contrast the results of Elkington et al. 2014, which indicate that rooting depth for oaks and junipers is not likely to extend past the shallow soil surface.

4.4 SPRING FLOW CHANGES FROM JUNIPER REMOVAL

Two different studies by Wilcox et al. (2008; 2010) showed either consistent or increases of baseflow in Nueces, Guadalupe, Llano, Frio, and the Concho River over the last ~85 years. Over this study period all sites have experienced woody plant encroachment of juniper and mesquite. They attribute the increase in baseflow to reduction in grazing hence improved range conditions, and increased infiltration and recharge due to the mix of vegetation suggesting that woody plant removal may not be needed on the scale of large rivers. Removal of juniper from watersheds that do not have a history of naturally existing spring flow did not result in an appearance of springs within the watersheds (Wilcox et al., 2005). Studies at scales of less than 20 ha have also seen an increase in recharge and spring flow (Wilcox et al., 2006, Wright, 1996). Huang et al. (2006) showed an increase in

streamflow post clearing of juniper by 46 mm year^{-1} . The increase in spring flow during this study is in agreement with a model created by Huxman et al. (2005), which indicated that in semi-arid landscapes stream/spring flow would only be impacted by woody plant (juniper) removal if preexisting flow existed. Therefore, if the goal of juniper removal is to increase spring flow then these studies indicate that it is feasible. Whereas if the goal is to have a spring appear in the area where one was not previously found the results are unlikely.

Additional juniper removal at this site may further increase available soil moisture and promote improved transpiration from other species. This additional clearing could potentially raise the water table and allow for additional shallow reservoirs to be filled to the benefit of more trees. In the wake of clearing, additional management will be necessary to prevent reestablishment of junipers in the cleared area from the large seed stocks left in the soil below the parent tree (M. K. Owens & Schliesing, 1995). Ranchers should likewise pay attention to the emergence of juniper seedlings along the canopy edges of mature trees left in the area from incomplete removal (Van Auken et al., 2005). The emphasis on additional management is important because juvenile junipers will increase water use after the clearing of larger trees as a result of the sudden reduction in competition (Moore & Owens, 2006).

Chapter 5: Conclusions

Our results indicate that pine transpired more on a per species basis than juniper and oak both pre- and post-clearing. However, it is likely that juniper would have the largest effect on site-scale water availability due to their larger numbers and lack in elevation preference at the site. The juniper removal in this study increased water availability indicated by increased amounts of transpiration by all species post clearing, and a visual increase of flow in the small spring at the bottom of the slope. Large oak trees experienced the greatest increase in transpiration following the clearing suggesting that water availability increased the most in their location. The absolute magnitude of increased water availability is uncertain due to the occurrence of drought. During drought, the large oaks were the only trees to continuously transpire, the large pines transpired further into the duration of the drought than the other pines and junipers, regardless of elevation.

We did not observe a consistent relationship between elevation and transpiration indicating a heterogeneous subsurface. Features such as rock fractures and preferential flow paths may play an important role in subsurface water dynamics along the slope. Large oaks and large pines located near potential preferential flow pathways benefitted the most from upslope juniper removal, as they were able to transpire longer and some of them continuously through drier conditions and drought. The increased water availability in these areas inferred by increased transpiration by large pines and large oaks could help prevent mortality in future droughts.

The extent and duration of additional water availability after clearing is uncertain due to reasons such as extended drought and vegetation reestablishment. In the study by Dugas et al. (1998), results initially indicated a decrease in evapotranspiration but after two years replacement grasses mitigated the effects of the juniper clearing. Therefore, future

management of juniper on this site should be mandated for two reasons. The first is that while mature juniper trees were removed, their seeds were not and could therefore reestablish (Owens & Schliesing, 1995). Juvenile juniper trees will increase transpiration and photosynthetic rates from lack of competition thus mitigating the effects of mature juniper removal (Van Auken et al., 2005). As climate changes via alterations in precipitation patterns and drought becoming more common an advanced understanding of how different plant species acquire, store, and use water will help us understand how ecosystems will react to these changes and give insight on land management best practices.

Appendix

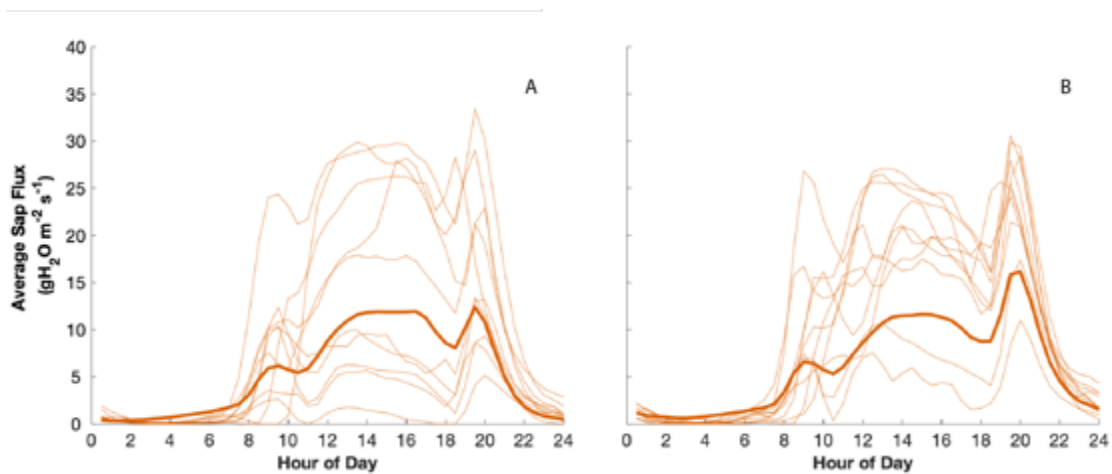


Figure 23: The average instantaneous sap flux over a diurnal period (dark orange) for juniper trees as seen in Figure 11 for 2018 (A) and 2019 (B) from DOY 120-300. The ten light orange lines are representative of varying patterns for diurnal curves from an individual tree responding to environmental conditions.

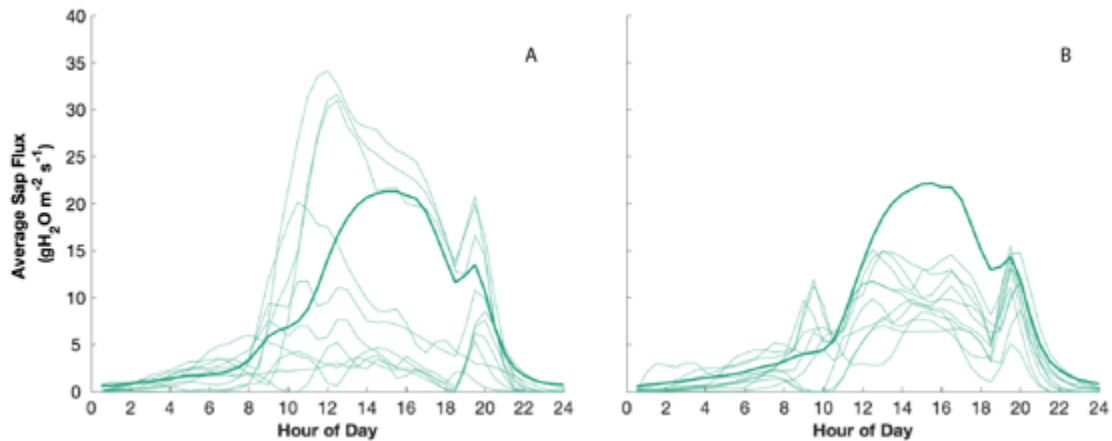


Figure 24: The average instantaneous sap flux over a diurnal period (dark green) for pine trees as seen in Figure 11 for 2018 (A) and 2019 (B) from DOY 120-300. The ten light green lines are representative of varying patterns for diurnal curves from an individual tree responding to environmental conditions.

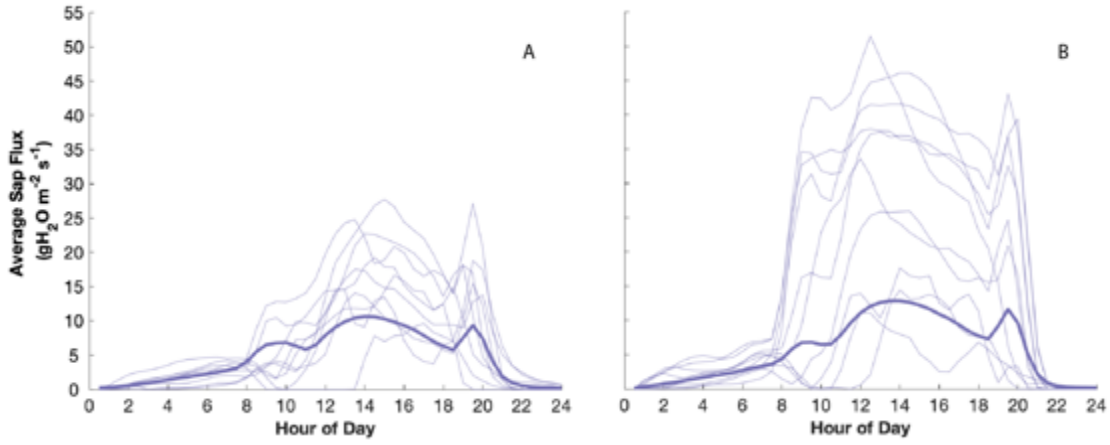


Figure 25: The average instantaneous sap flux over a diurnal period (dark blue) for oak trees as seen in Figure 11 for 2018 (A) and 2019 (B) from DOY 120-300. The ten light blue lines are representative of varying patterns for diurnal curves from an individual tree responding to environmental conditions.

References

- Abrams, M. D. (1992). Fire and the Development of Oak Forests. *BioScience*, 42(5), 346–353. <https://doi.org/10.2307/1311781>
- Aro, R. (1983). Pinyon-juniper. *Silvicultural Systems for the Major Forest Types of the United States*, 84–86.
- Auken, O. W. Van. (2000). S Emiarid G Rasslands. *Annual Review Ecological Systematic*, 31, 197–215.
- Bray, W. (1904). *The timber of the Edwards Plateau of Texas; its relation to climate, water supply, and soil.*
- Bryant, F. C., Launchbaugh, G. K., & Koerth, B. H. (1983). Controlling Mature Ashe Juniper in Texas with Crown Fires. *Journal of Range Management*, 36(2), 165. <https://doi.org/10.2307/3898154>
- Burkhardt, J. W., & Tisdale, E. W. (1976). *Causes of Juniper Invasion in Southwestern Idaho*. 57(3), 472–484.
- Cardella Dammeyer, H., Schwinning, S., Schwartz, B. F., & Moore, G. W. (2016). Effects of juniper removal and rainfall variation on tree transpiration in a semi-arid karst: evidence of complex water storage dynamics. *Hydrological Processes*, 30(24), 4568–4581. <https://doi.org/10.1002/hyp.10938>
- Chemura, A., Rwasoka, D., Mutanga, O., Dube, T., & Mushore, T. (2020). The impact of land-use/land cover changes on water balance of the heterogeneous Buzi sub-catchment, Zimbabwe. *Remote Sensing Applications: Society and Environment*, 18, 100292. <https://doi.org/10.1016/j.rsase.2020.100292>
- Davis, T. W., Kuo, C. M., Liang, X., & Yu, P. S. (2012). Sap flow sensors: Construction, quality control and comparison. *Sensors*, 12(1), 954–971. <https://doi.org/10.3390/s120100954>
- Dugas, W. a., Hicks, R. a., & Wright, P. (1998). on evapotranspiration and runoff in the Seco Creek Watershed. *Water Resources Research*, 34(6), 1499. <https://doi.org/10.1029/98WR00556>
- Eldridge, D. J., Delgado-Baquerizo, M., Travers, S. K., Val, J., & Oliver, I. (2017). Do grazing intensity and herbivore type affect soil health? Insights from a semi-arid productivity gradient. *Journal of Applied Ecology*, 54(3), 976–985. <https://doi.org/10.1111/1365-2664.12834>
- Elkington, R. J., Rebel, K. T., Heilman, J. L., Litvak, M. E., Dekker, S. C., & Moore, G. W. (2014). Species-specific water use by woody plants on the Edwards Plateau, Texas. *Ecohydrology*, 7(2), 278–290. <https://doi.org/10.1002/eco.1344>
- EPRON, D., & DREYER, E. (1993). Long-term effects of drought on photosynthesis of adult oak trees [*Quercus petraea* (Matt.) Liebl. and *Quercus robur* L.] in a natural stand. *New Phytologist*, 125(2), 381–389. <https://doi.org/10.1111/j.1469-8137.1993.tb03890.x>
- Estrada-Medina, H., Graham, R. C., Allen, M. F., Jiménez-Osornio, J. J., & Robles-Casolco, S. (2013). The importance of limestone bedrock and dissolution karst features on tree root distribution in northern Yucatán, México. *Plant and Soil*,

- 362(1–2), 37–50. <https://doi.org/10.1007/s11104-012-1175-x>
- Fies, J. C., De Louvigny, N., & Chanzy, A. (2002). The role of stones in soil water retention. *European Journal of Soil Science*, *53*(1), 95–104. <https://doi.org/10.1046/j.1365-2389.2002.00431.x>
- Fisher, J. B., Baldocchi, D. D., Misson, L., Dawson, T. E., & Goldstein, A. H. (2007). What the towers don't see at night: Nocturnal sap flow in trees and shrubs at two AmeriFlux sites in California. *Tree Physiology*, *27*(4), 597–610. <https://doi.org/10.1093/treephys/27.4.597>
- Fuhrendorf, S. D., Smeins, F. E., & Grant, W. E. (1996). Simulation of a fire-sensitive ecological threshold: A case study of Ashe juniper on the Edwards Plateau of Texas, United States. *Ecological Modelling*, *90*(3), 245–255. [https://doi.org/10.1016/0304-3800\(95\)00151-4](https://doi.org/10.1016/0304-3800(95)00151-4)
- GRANIER, A., & GROSS, P. (1987). Mesure du flux de sève brute dans le tronc du Douglas par une nouvelle méthode thermique. *Annales Des Sciences Forestières*, *44*(1), 1–14. <https://doi.org/10.1051/forest:19870101>
- Heilman, J. L., McInnes, K. J., Kjelgaard, J. F., Keith Owens, M., & Schwinning, S. (2009). Energy balance and water use in a subtropical karst woodland on the Edwards Plateau, Texas. *Journal of Hydrology*, *373*(3–4), 426–435. <https://doi.org/10.1016/j.jhydrol.2009.05.007>
- Honda, E. A., & Durigan, G. (2016). Woody encroachment and its consequences on hydrological processes in the savannah. *Philosophical Transactions of the Royal Society B: Biological Sciences*, *371*(1703). <https://doi.org/10.1098/rstb.2015.0313>
- Houghton, R., Connors, S., & Krinner, G. (n.d.). *Land–climate interactions*.
- Huxman, T. E., Wilcox, B. P., Breshears, D. D., Scott, R. L., Snyder, K. A., Small, E. E., Hultine, K., Pockman, W. T., & Jackson, R. B. (2005). Ecohydrological implications of woody plant encroachment. *Ecology*, *86*(2), 308–319. <https://doi.org/10.1890/03-0583>
- Jackson, R. B., Moore, L. A., Hoffmann, W. A., Pockman, W. T., & Linder, C. R. (1999). Ecosystem rooting depth determined with caves and DNA. *Proceedings of the National Academy of Sciences of the United States of America*, *96*(20), 11387–11392. <https://doi.org/10.1073/pnas.96.20.11387>
- Jasechko, S., Sharp, Z. D., Gibson, J. J., Birks, S. J., Yi, Y., & Fawcett, P. J. (2013). Terrestrial water fluxes dominated by transpiration. *Nature*, *496*(7445), 347–350. <https://doi.org/10.1038/nature11983>
- Keys, P. W., Barnes, E. A., Van Der Ent, R. J., & Gordon, L. J. (2014). Variability of moisture recycling using a precipitationshed framework. *Hydrology and Earth System Sciences*, *18*(10), 3937–3950. <https://doi.org/10.5194/hess-18-3937-2014>
- Kukowski, K. R., Schwinning, S., & Schwartz, B. F. (2013). Hydraulic responses to extreme drought conditions in three co-dominant tree species in shallow soil over bedrock. *Oecologia*, *171*(4), 819–830. <https://doi.org/10.1007/s00442-012-2466-x>
- Macfarlane, C., Bond, C., White, D. A., Grigg, A. H., Ogden, G. N., & Silberstein, R. (2010). Transpiration and hydraulic traits of old and regrowth eucalypt forest in southwestern Australia. *Forest Ecology and Management*, *260*(1), 96–105.

- <https://doi.org/10.1016/j.foreco.2010.04.005>
- McCole, A. A., & Stern, L. A. (2007). Seasonal water use patterns of *Juniperus ashei* on the Edwards Plateau, Texas, based on stable isotopes in water. *Journal of Hydrology*, 342(3–4), 238–248. <https://doi.org/10.1016/j.jhydrol.2007.05.024>
- McDowell, N., Pockman, W. T., Allen, C. D., Breshears, D. D., Cobb, N., Kolb, T., Plaut, J., Sperry, J., West, A., Williams, D. G., & Yepez, E. A. (2008). Mechanisms of plant survival and mortality during drought: Why do some plants survive while others succumb to drought? *New Phytologist*, 178(4), 719–739. <https://doi.org/10.1111/j.1469-8137.2008.02436.x>
- Moore, G. W., Bond, B. J., Jones, J. A., Phillips, N., & Meinzer, F. C. (2004). Structural and compositional controls on transpiration in 40- and 450-year-old riparian forests in western Oregon, USA. *Tree Physiology*, 24(5), 481–491. <https://doi.org/10.1093/treephys/24.5.481>
- Moore, G. W., & Owens, M. K. (2006). Removing adult overstory trees stimulates growth and transpiration of conspecific juvenile trees. *Rangeland Ecology and Management*, 59(4), 416–421. [https://doi.org/10.2111/1551-5028\(2006\)59\[416:RAOTSG\]2.0.CO;2](https://doi.org/10.2111/1551-5028(2006)59[416:RAOTSG]2.0.CO;2)
- Nadezhdina, N. (1999). Sap flow index as an indicator of plant water status. *Tree Physiology*, 19(13), 885–891. <https://doi.org/10.1093/treephys/19.13.885>
- Oishi, A. C., Hawthorne, D. A., & Oren, R. (2016). Baseline: An open-source, interactive tool for processing sap flux data from thermal dissipation probes. *SoftwareX*, 5, 139–143. <https://doi.org/10.1016/j.softx.2016.07.003>
- Oishi, A. C., Oren, R., & Stoy, P. C. (2008). Estimating components of forest evapotranspiration: A footprint approach for scaling sap flux measurements. *Agricultural and Forest Meteorology*, 148(11), 1719–1732. <https://doi.org/10.1016/j.agrformet.2008.06.013>
- Oki, T., & Kanae, S. (2006). *Oki and Kanae 2006 Global Hydrological cycles and World water resources.pdf*. August, 1068–1072.
- Owens, M. K. (1996). The role of leaf and canopy-level gas exchange in the replacement of *Quercus virginiana* (Fagaceae) by *Juniperus ashei* (Cupressaceae) in semiarid savannas. *American Journal of Botany*, 83(5), 617–623. <https://doi.org/10.1002/j.1537-2197.1996.tb12747.x>
- Owens, M. K., & Schliesing, T. G. (1995). Invasive potential of ashe juniper after mechanical disturbance. *Journal of Range Management*, 48(6), 503–507. <https://doi.org/10.2307/4003060>
- Owens, M. Keith, Lyons, R. K., & Alejandro, C. (2006). Rainfall partitioning within semiarid juniper communities: effects of event size and canopy cover. *HYDROLOGICAL PROCESSES*, 20, 3179–3189. <https://doi.org/10.1002/hyp>
- Pangle, R. E., Limousin, J. M., Plaut, J. A., Yepez, E. A., Hudson, P. J., Boutz, A. L., Gehres, N., Pockman, W. T., & McDowell, N. G. (2015). Prolonged experimental drought reduces plant hydraulic conductance and transpiration and increases mortality in a piñon-juniper woodland. *Ecology and Evolution*, 5(8), 1618–1638. <https://doi.org/10.1002/ece3.1422>

- Rawls, W. J., Brakensiek, D. L., & Saxton, K. E. (1982). Rawls et al 1982.pdf. In *Transactions of the ASAE* (Vol. 25, Issue 5, pp. 1316–1320 & 1328).
<http://www.envsci.rutgers.edu/~gimenez/SoilPhysics/Homework08/Rawls et al 1982.pdf>
- Reemts, C. M., & Hansen, L. L. (2008). Slow recolonization of burned oak-juniper woodlands by Ashe juniper (*Juniperus ashei*): Ten years of succession after crown fire. *Forest Ecology and Management*, 255(3–4), 1057–1066.
<https://doi.org/10.1016/j.foreco.2007.10.013>
- Russell, F. L., & Fowler, N. L. (2004). Effects of white-tailed deer on the population dynamics of acorns, seedlings and small saplings of *Quercus buckleyi*. *Plant Ecology*, 173(1), 59–72. <https://doi.org/10.1023/B:VEGE.0000026329.47461.99>
- Sankey, T. T., & Germino, M. J. (2008). Assessment of juniper encroachment with the use of satellite imagery and geospatial data. *Rangeland Ecology and Management*, 61(4), 412–418. <https://doi.org/10.2111/07-141.1>
- Schlesinger, W. H., & Jasechko, S. (2014). Transpiration in the global water cycle. *Agricultural and Forest Meteorology*, 189–190, 115–117.
<https://doi.org/10.1016/j.agrformet.2014.01.011>
- Schwinning, S. (2008). *The Water Relations of Two Evergreen Tree Species in a Karst Savanna*. 158(3), 373–383.
- Soil Survey Staff, U. (2017). *Web soil survey*.
- Sperry, J. S., Tyree, M. T., Sperry, J. S., & Tyree, M. T. (1988). *Mechanism of Water Stress-Induced Xylem Embolism*. 88(3), 581–587.
- Starks, P. J., Venuto, B. C., Dugas, W. A., & Kiniry, J. (2014). Measurements of canopy interception and transpiration of openly-grown eastern redcedar in central Oklahoma. *Environment and Natural Resources Research*, 4(3).
<https://doi.org/10.5539/enrr.v4n3p103>
- Thurrow, A. T. L., Blackburn, W. H., Warren, S. D., & Taylor, C. A. (2018). *Society for Range Management Rainfall Interception by Midgrass, Shortgrass, and Live Oak Mottes Published by: Society for Range Management Stable URL: <http://www.jstor.org/stable/3899611> Linked references are available on JSTOR for this article: Rain*. 40(5), 455–460.
- Tokumoto, I., Heilman, J. L., Schwinning, S., McInnes, K. J., Litvak, M. E., Morgan, C. L. S., & Kamps, R. H. (2014). Small-scale variability in water storage and plant available water in shallow, rocky soils. *Plant and Soil*, 385(1–2), 193–204.
<https://doi.org/10.1007/s11104-014-2224-4>
- Tyree, M., & Cochard, H. (1996). Summer and winter embolism in oak: impact on water relations. *Annales Des Sciences Forestières*, 53(2–3), 173–180.
<https://doi.org/10.1051/forest:19960201>
- Van Auken, O. W., Jackson, J. T., & Jurena, P. N. (2005). Survival and growth of *Juniperus* seedlings in *Juniperus* woodlands. *Plant Ecology*, 175(2), 245–257.
<https://doi.org/10.1007/s11258-005-0022-z>
- Ward, D., Hoffman, M. T., & Collocott, S. J. (2014). A century of woody plant encroachment in the dry Kimberley savanna of South Africa. *African Journal of*

- Range and Forage Science*, 31(2), 107–121.
<https://doi.org/10.2989/10220119.2014.914974>
- West, A. G., Hultine, K. R., Burtch, K. G., & Ehleringer, J. R. (2007). Seasonal variations in moisture use in a piñon-juniper woodland. *Oecologia*, 153(4), 787–798.
<https://doi.org/10.1007/s00442-007-0777-0>
- West, A. G., Hultine, K. R., Sperry, J. S., Bush, S. E., & Ehleringer, J. R. (2008). Transpiration and hydraulic strategies in a piñon-juniper woodland. *Ecological Applications*, 18(4), 911–927. <https://doi.org/10.1890/06-2094.1>
- Wilcox, B. P., & Huang, Y. (2010). Woody plant encroachment paradox: Rivers rebound as degraded grasslands convert to woodlands. *Geophysical Research Letters*, 37(7), 1–6. <https://doi.org/10.1029/2009GL041929>
- Wilcox, B. P., Huang, Y., & Walker, J. W. (2008). Long-term trends in streamflow from semiarid rangelands: Uncovering drivers of change. *Global Change Biology*, 14(7), 1676–1689. <https://doi.org/10.1111/j.1365-2486.2008.01578.x>
- Wilcox, B. P., Owens, M. K., Knight, R. W., & Lyons, R. K. (2005). Do woody plants affect streamflow on semiarid karst rangelands? *Ecological Applications*, 15(1), 127–136. <https://doi.org/10.1890/04-0664>
- Wilcox, B. P., Sorice, M. G., Angerer, J., & Wright, C. L. (2012). Historical changes in stocking densities on texas rangelands. *Rangeland Ecology and Management*, 65(3), 313–317. <https://doi.org/10.2111/REM-D-11-00119.1>
- Wilcox Bradford P., Owens M., Dugas Williams, Ueckert Darrel, H. C. (2006). Shrubs, streamflow, and the paradox of scale. *HYDROLOGICAL PROCESSES*, 20(November 2008), 3245–3259. <https://doi.org/10.1002/hyp>
- Wong, C., & Banner, J. L. (2010). Response of cave air CO₂ and drip water to brush clearing in central Texas: Implications for recharge and soil CO₂ dynamics. *Journal of Geophysical Research: Biogeosciences*, 115(4).
<https://doi.org/10.1029/2010JG001301>
- Xu, L., & Baldocchi, D. D. (2003). Seasonal trends in photosynthetic parameters and stomatal conductance of blue oak (*Quercus douglasii*) under prolonged summer drought and high temperature. *Tree Physiology*, 23(13), 865–877.
<https://doi.org/10.1093/treephys/23.13.865>
- Yao, J., Murray, D. B., Adhikari, A., & White, J. D. (2012). Fire in a sub-humid woodland: The balance of carbon sequestration and habitat conservation. *Forest Ecology and Management*. <https://doi.org/10.1016/j.foreco.2012.05.042>
- Yun Huang, 1* Bradford P. Wilcox, 1 Libby Stern² and Humberto Perotto-Baldivieso¹. (2006). Springs on rangelands: runoff dynamics and influence of. *HYDROLOGICAL PROCESSES*, 20(october 2006), 3277–3288. <https://doi.org/10.1002/hyp>
- Zou, C. B., Turton, D. J., Will, R. E., Engle, D. M., & Fuhlendorf, S. D. (2014). Alteration of hydrological processes and streamflow with juniper (*Juniperus virginiana*) encroachment in a mesic grassland catchment. *Hydrological Processes*, 28(26), 6173–6182. <https://doi.org/10.1002/hyp.10102>